ERMABI – Exploiting the Resilience of Masonry Arch Bridge Infrastructure

University of Sheffield

Imperial College London

A 3D discrete-macro-element-method for the structural assessment of masonry bridges

Prof. Ivo Caliò

Università di Catania

DICAR Dipartimento Ingegneria Civile e Architettura

Nonlinear Modeling of masonry structures

Detailed modeling of masonry considering its constituents is today hardly applicable in practical applications to the simulation of entire structures due to the computational cost it entails.

- Simplified models are adopted especially for masonry buildings to predict global box-type behavior while out-of-plane response is generally evaluated separately according to local mechanisms through limit analysis approaches.
- For masonry bridges both simplified and accurate models can be adopted. However, in order to account for the contribution of all the structural as well as nonstructural elements, geometrically consistent models should be adopted for assessing the existing bridge structural performance up to collapse conditions.

The macro-element strategy for unreinforced masonry buildings

Each wall of the building is sub-divided into macro-portion (identified as macro-elements) whose behavior is globally described by ad hoc equivalent structural element

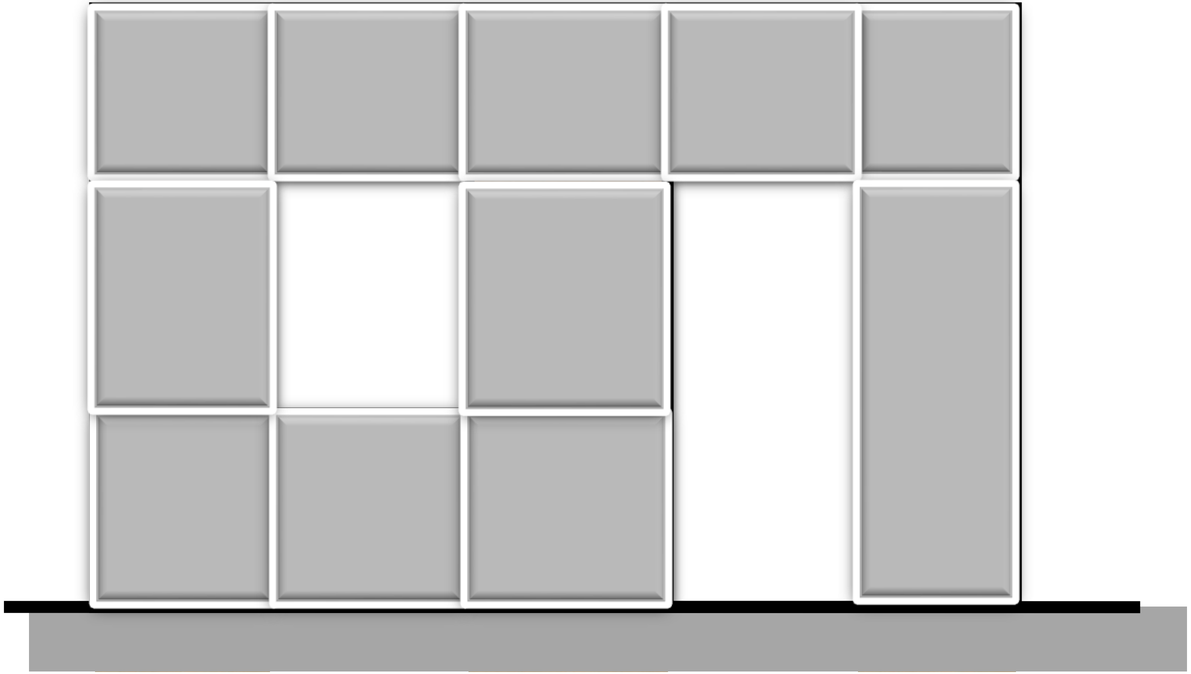

The Equivalent Frame Model (EFM)

The equivalent frame model is currently widely used in the engineering practice for masonry building.

A plane masonry walls is represented by an equivalent nonlinear frame

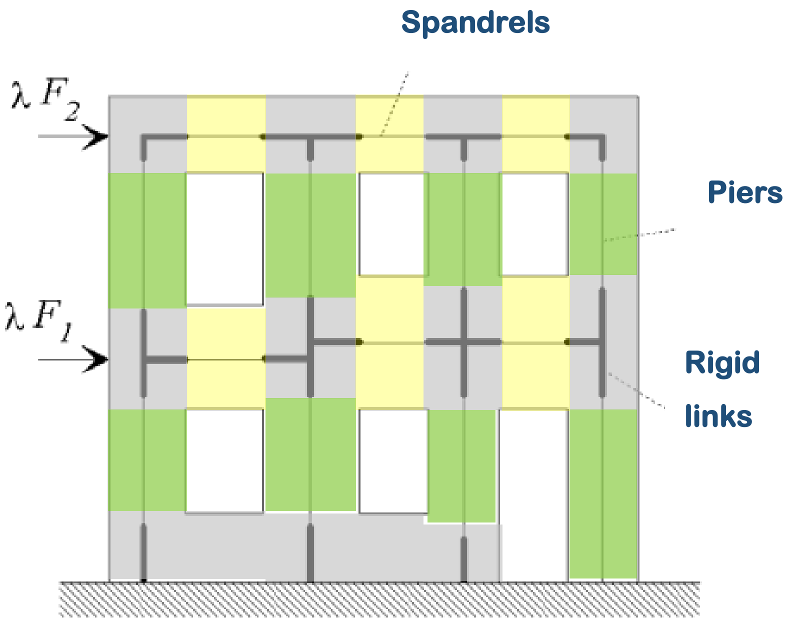

Several approaches have been proposed in the literature.

In the EFM it is generally assumed that in-plane damage can occur on piers and spandrels while the other masonry portion are not subjected to damage.

Magenes, G, & Della Fontana, A 1998, 'Simplified nonlinear seismic analysis of masonry buildings', British Masonry Society Proceedings, no. 8, pp. 190–195.

Raka, E, Spacone, E, Sepe, V, & Camata, G 2015, 'Advanced frame element for seismic analysis of masonry structures: model formulation and validation', Earthquake Engineering and Structural Dynamics, vol. 44, pp. 2489–2506, doi:10.1002/eqe.2594.

Lagomarsino, S., Penna, A., Galasco, A., and Cattari, S. (2013). TREMURI program: an equivalent frame model for the nonlinear seismic analysis of masonry buildings. Eng. Struct. 56, 1787–1799. doi:10.1016/j.engstruct.2013.08.002.

The discrete macro element method for masonry buildings

The DMEM has been initially proposed as an alternative to the frame models for the assessment of masonry buildings

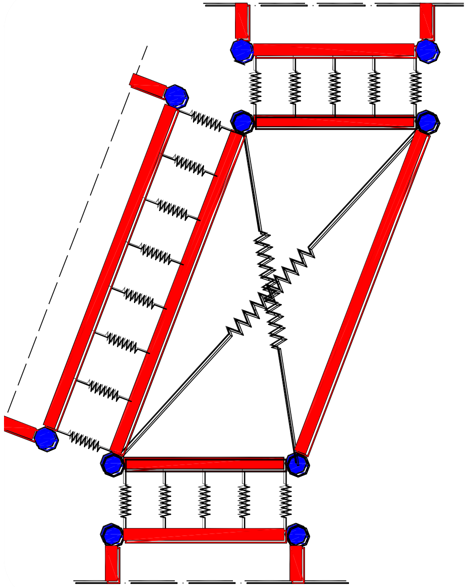

Articulated quadrilateral

Two diagonal NLinks

A discrete distributions of Nlinks

which connect the adjacent elements

[1] I. Caliò, M. Marletta, B. Pantò 2005. A simplified model for the evaluation of the seismic behaviour of masonry buildings. 10th International Conference on Civil, Structural and Environmental Engineering Computing, Rome

[2] I. Caliò, M. Marletta, B. Pantò 2012. A new discrete element model for the evaluation of the seismic behaviour of unreinforced masonry buildings. Engineering Structures 40 327–338.

The in-plane failure mechanisms

rocking

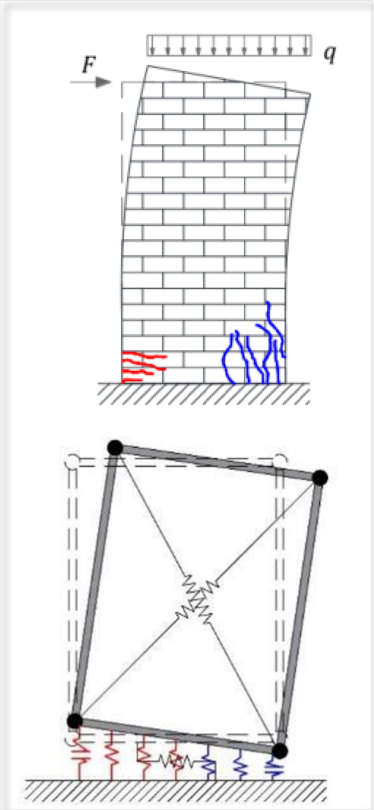

Shear-diagonal

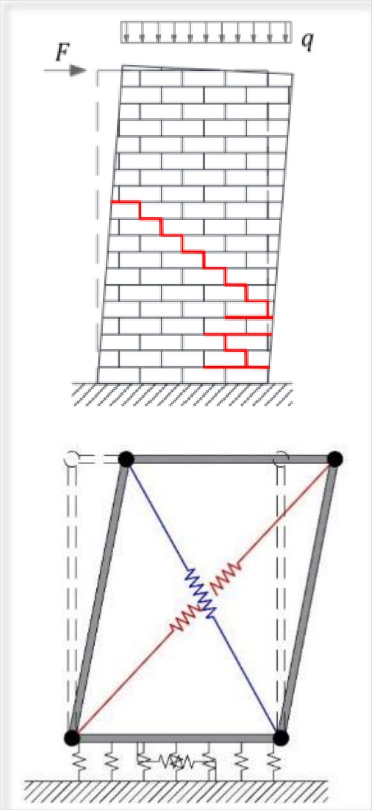

sliding

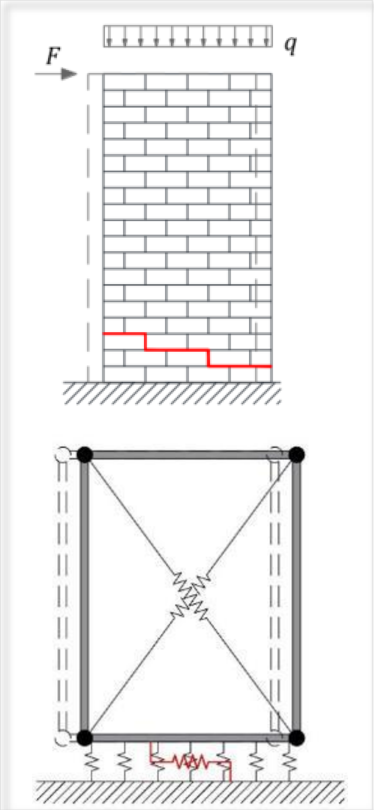

The kinematics

The kinematics is governed by 4 degrees of freedom only

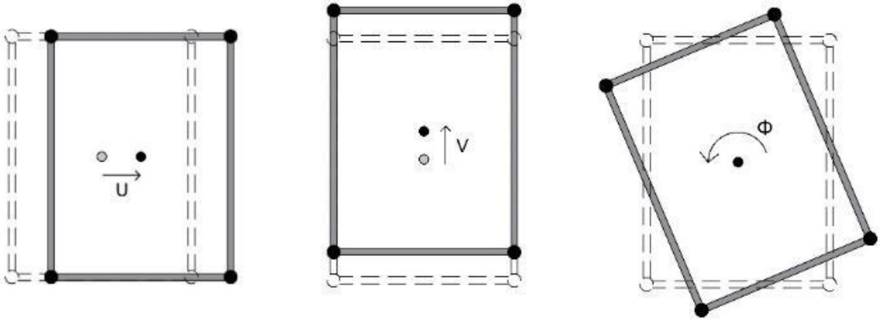

3 degrees related to the rigid motion

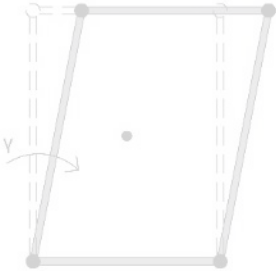

1 degree for the shear deformation

MACRO-ELEMENTO PIANO

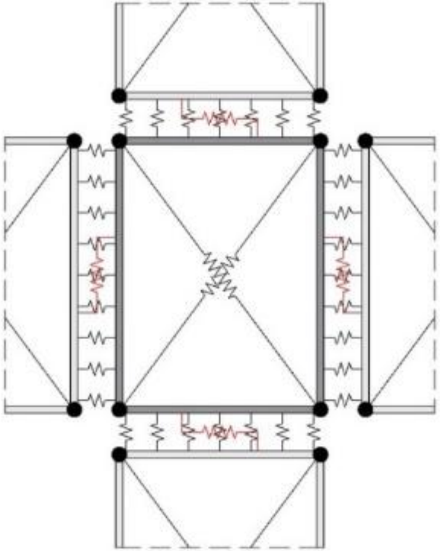

I. Caliò, M. Marletta, and B. Pantò, "A new discrete element model for the evaluation of the seismic behaviour of unreinforced masonry buildings," Engineering Structures, vol. 40, pp. 237-338, (2012).

The origin of the DMEM for assessing the global behavior of masonry buildings

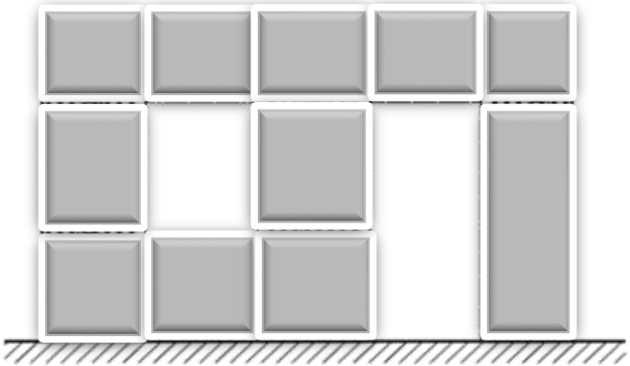

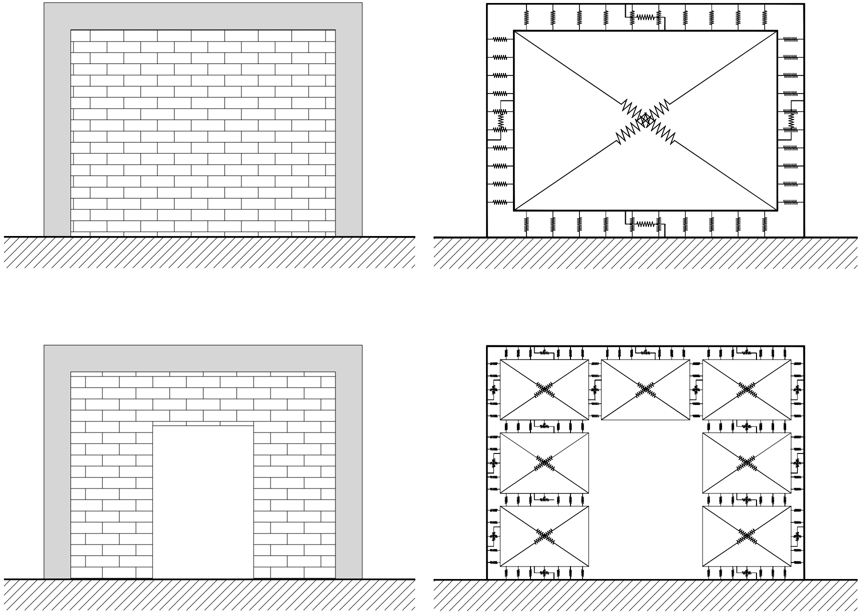

I. Caliò, M. Marletta, and B. Pantò, "A new discrete element model for the evaluation of the seismic behaviour of unreinforced masonry buildings," Engineering Structures, vol. 40, pp. 237-338, (2012).

The definition of the mechanical properties of Nlinks

(simple example relative to an infilled frame)

The mechanical properties of the Nlinks orthogonal to the interfaces

The calibration of the nonlinear links orthogonal to the interfaces follows a simple fiber strategy

The number of nonlinear links considered does not influence the number of the needed degrees of freedom

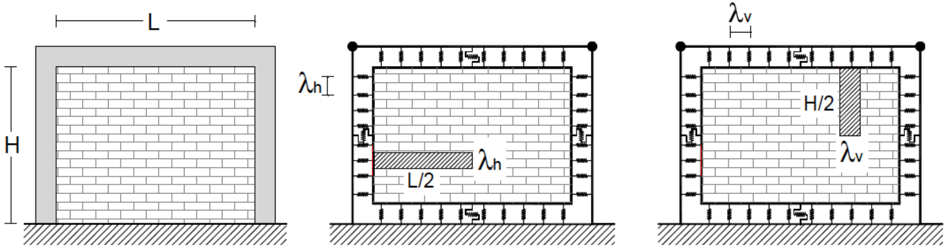

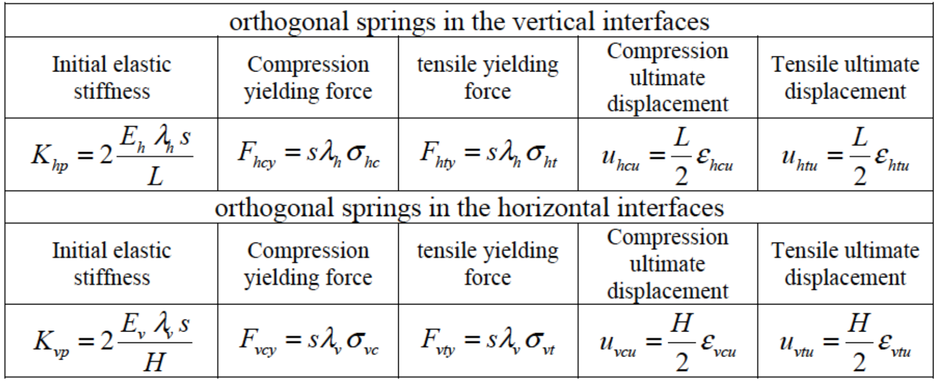

orthogonal springs in the vertical interfaces				
Initial elastic stiffness	Compression yielding force	tensile yielding force	Compression ultimate displacement	Tensile ultimate displacement
$K_{hp} = 2\frac{E_h \lambda_h s}{L}$	$F_{hcy} = s\lambda_h \sigma_{hc}$	$F_{hty} = s\lambda_h \sigma_{ht}$	$u_{hcu} = \frac{L}{2}\varepsilon_{hcu}$	$u_{htu} = \frac{L}{2}\varepsilon_{htu}$
orthogonal springs in the horizontal interfaces				
Initial elastic stiffness	Compression yielding force	tensile yielding force	Compression ultimate displacement	Tensile ultimate displacement
$K_{vp} = 2\frac{E_v \lambda_v s}{H}$	$F_{vcy} = s\lambda_v \sigma_{vc}$	$F_{vty} = s\lambda_v \sigma_{vt}$	$u_{vcu} = \frac{H}{2}\varepsilon_{vcu}$	$u_{vtu} = \frac{H}{2}\varepsilon_{vtu}$

The discrete macro-element for plane masonry arches

The approach has been extended to plane masonry arches by considering a quadrilater with irregular geometry

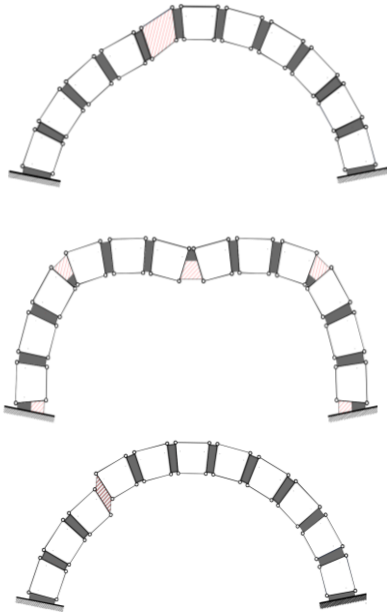

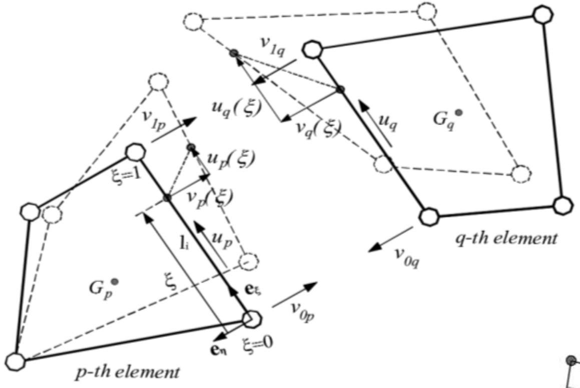

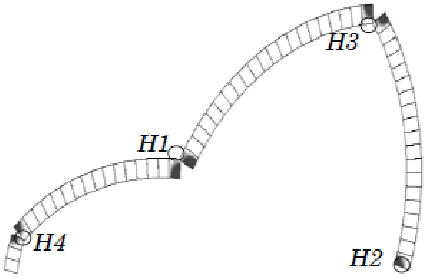

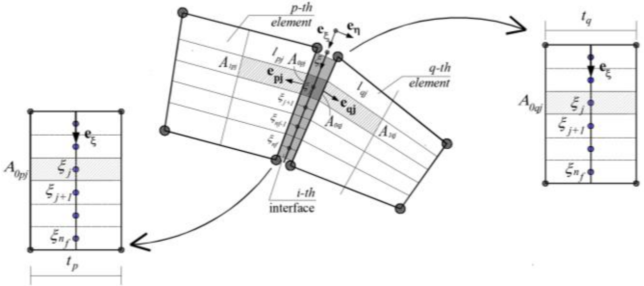

F. Cannizzaro, B. Pantò, S. Caddemi, I. Caliò. A Discrete Macro-Element Method (DMEM) for the nonlinear structural assessment of masonry arches. *Engineering Structures (2018) 168:243-256327–338.*

Practical engineering applications

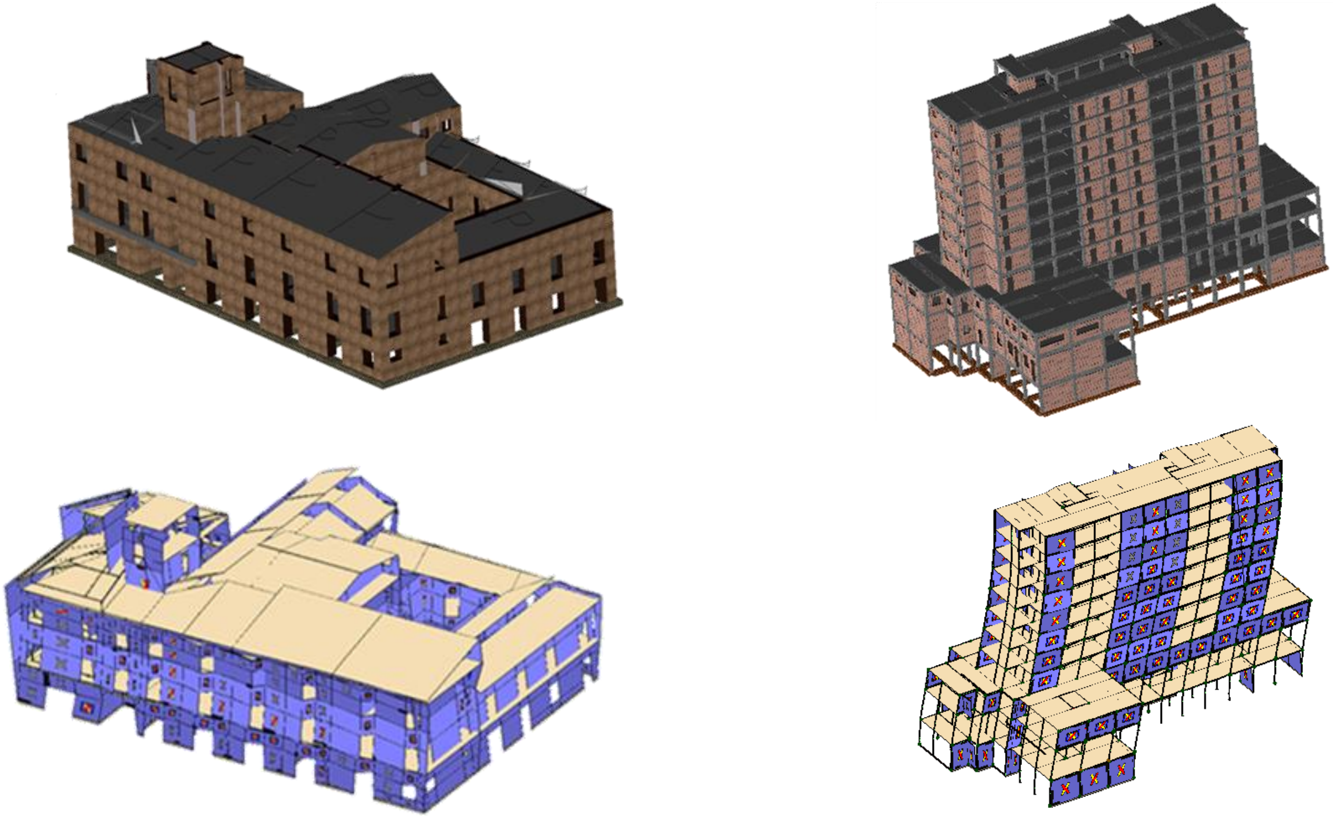

3DMACRO
FOR EXISTING BUILDINGS

The first macro-element including the out-of-plane behaviour

B. Pantò – PhD thesis 2007

In the plane macroelement, the out-of-plane behavior is ignored.

This restriction was removed by adding a third dimension

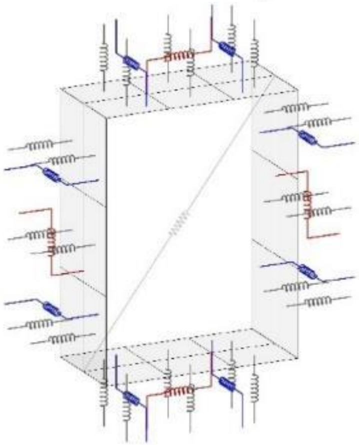

Il macro-elemento spaziale

Three additional degrees of freedom are necessary for the description of the out-of-plane kinematics and additional nonlinear links take into account the three-dimensional mechanical behavior

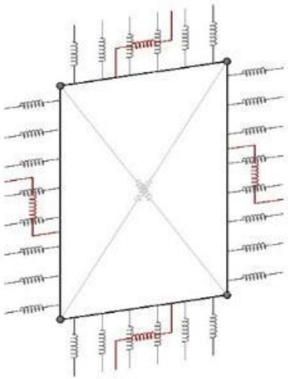

The plane macro-element

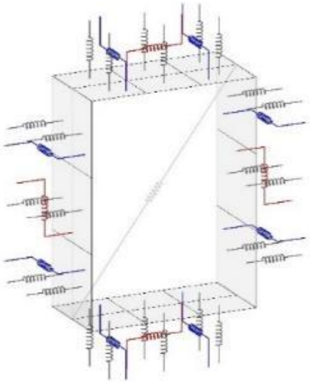

The spatial macro-element

Experimental and Numerical Validation

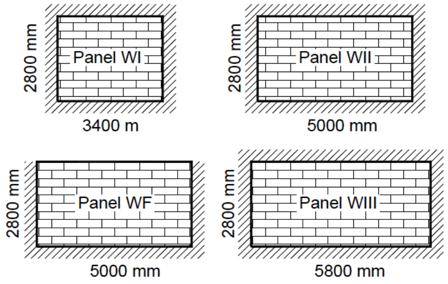

Figure 6 - Geometry of the tested panels, Gazzola et al (1985) [3]. Dimensions in mm.
All the panels have the same height (2800 mm) and thickness (100 mm) but different aspect ratio:

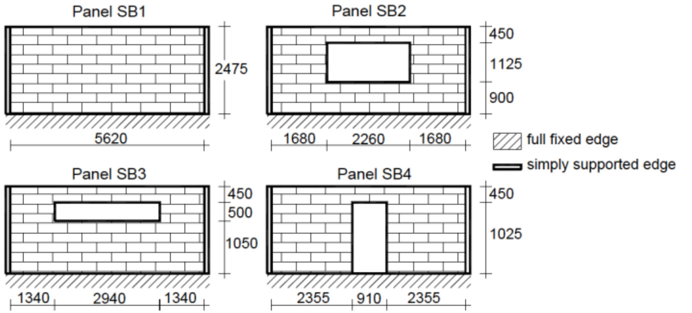

Figure 11: Geometry of the panels with different opening sizes, Chong et al (1995). Dimensions in

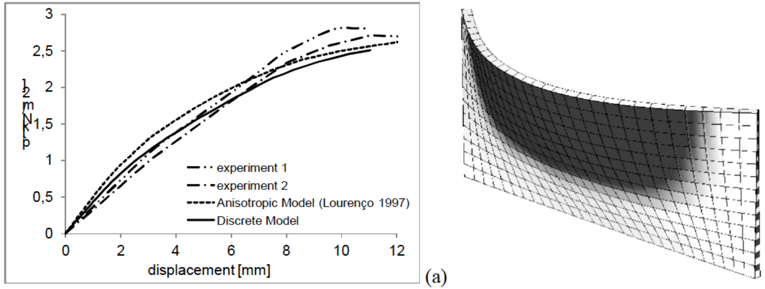

(b)Figure 12 - Panel SB1: (a) force-displacement diagram; (b) collapse mechanism and damage scenario in term of cumulated inelastic energy at the last step.

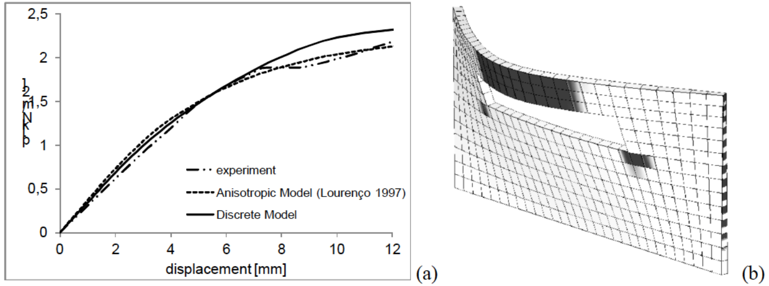

Figure 14 - Panel SB3: (a) force-displacement curve; (b) collapse mechanism and damage scenario in term of cumulated inelastic energy at the last step.

B. Pantò, I. Caliò, P.B. Lourenco, 'Numerical and experimental validation of a 3D macro-model for the in-plane and out-of-plane behaviour of unreinforced masonry walls', paper under review.

Application to a Basilica Plan Church

Numerical simulation of a Basilica Plan Church

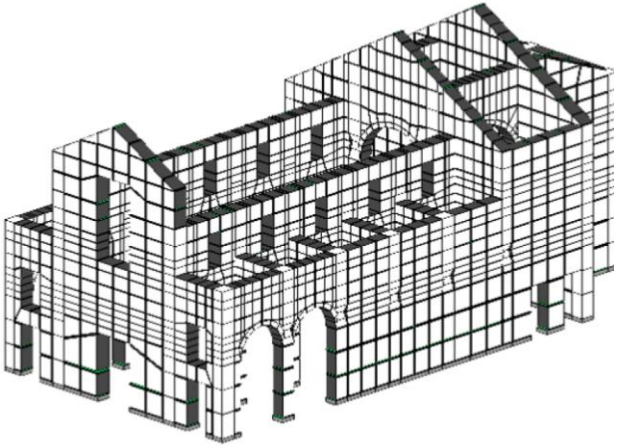

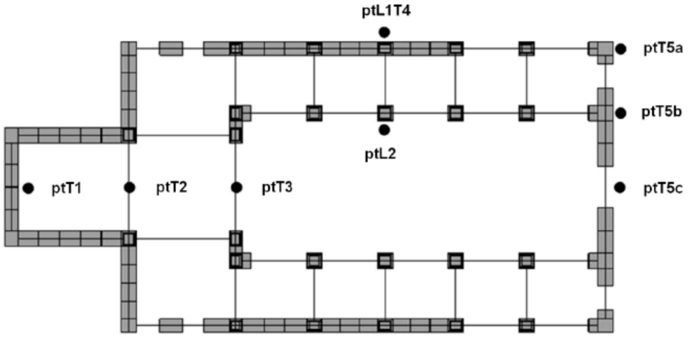

Pantò, E., F. Cannizzaro, S. Caddemi, I. Caliò, "3D macro-element modelling approach for seismic assessment of historical masonry churches", Advances in engineering softwares 97 (2016) 40-59.

Application to a Basilica Plan Church

Mass-proportional push-over analysis in the longitudinal direction

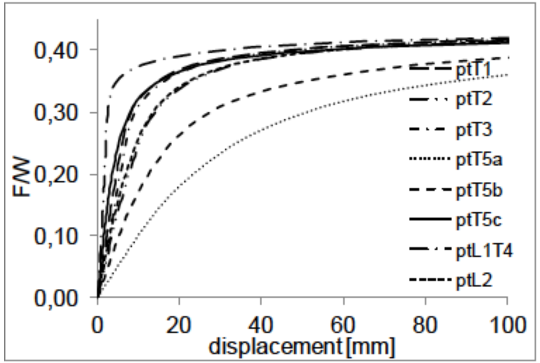

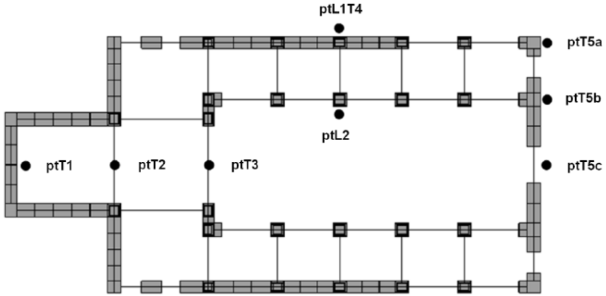

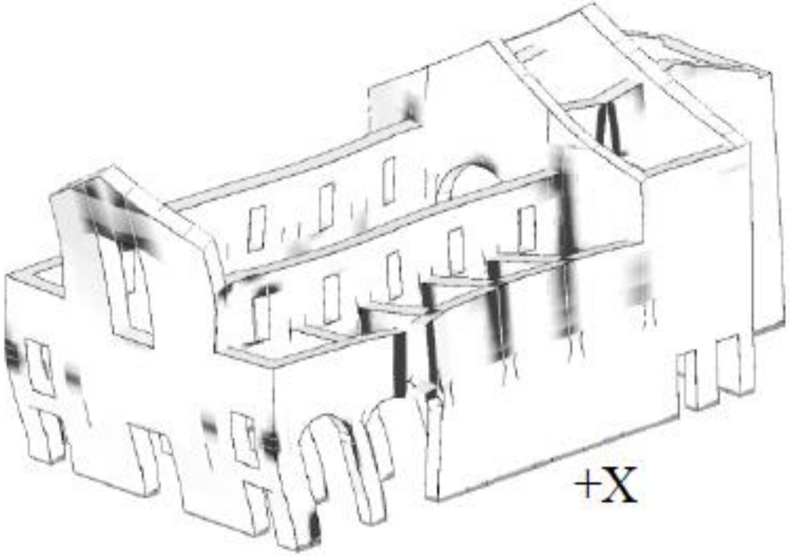

The first macro-element for modelling curved-geometry

A macro-element for vaulted structures

F. Cannizzaro – PhD thesis 2011

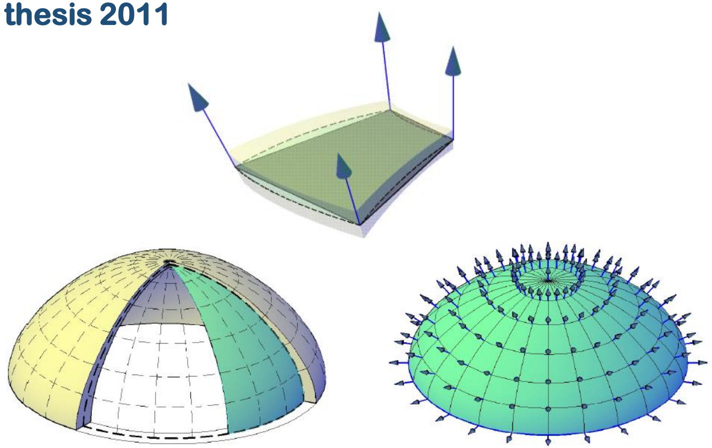

Each macro-element is characterised by four rigid layer edges whose orientation and dimension is associated to the shape of the element and to the thickness of the portion of masonry that must be represented.

From the structure to its macro-model representation

A curved geometry structure is discretized by means of an assemblage of several flat elements.

- **each element possesses only 7 degrees of freedom**
- **The geometry of the macro-element is irregular**
- **The interfaces are not orthogonal to the plane of the element**
- **the assumption of constant thickness has been removed allowing for the modeling of variable thickness structures**

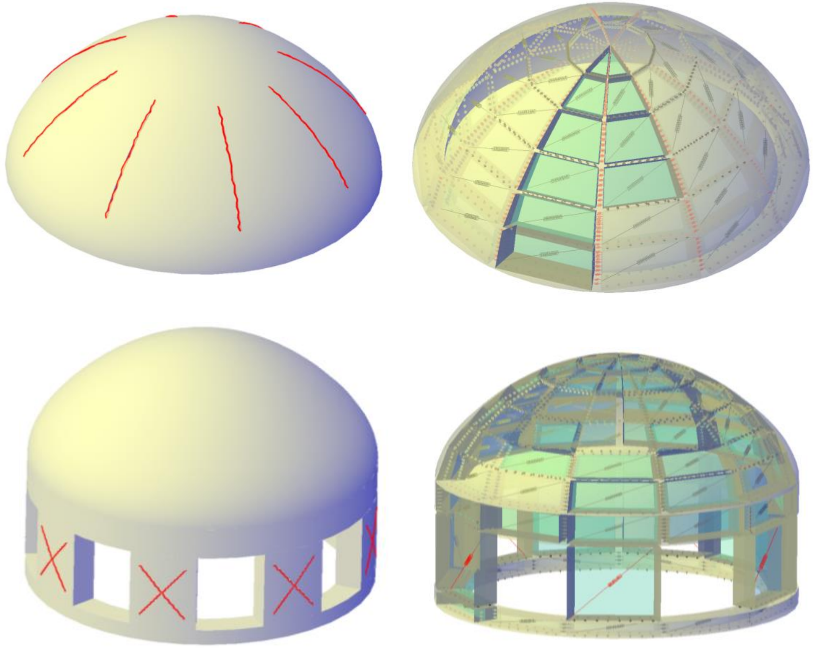

The macro-element approach extended to nonlinear dynamic time-history analyses

Chácara C – PhD thesis 2018

César Chácara Espinoza – University of Minho. Macro-Element Nonlinear Dynamic Analysis for the Assessment of the Seismic Vulnerability of Masonry Structures Supervisors prof Paulo Lourenco, prof Ivo Caliò

Experimental and numerical validation

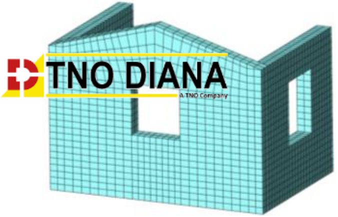

**Finite Element model
(54,477 DOFs)**

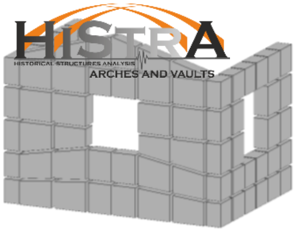

**Discrete Macro-element model
(616 DOFs)**

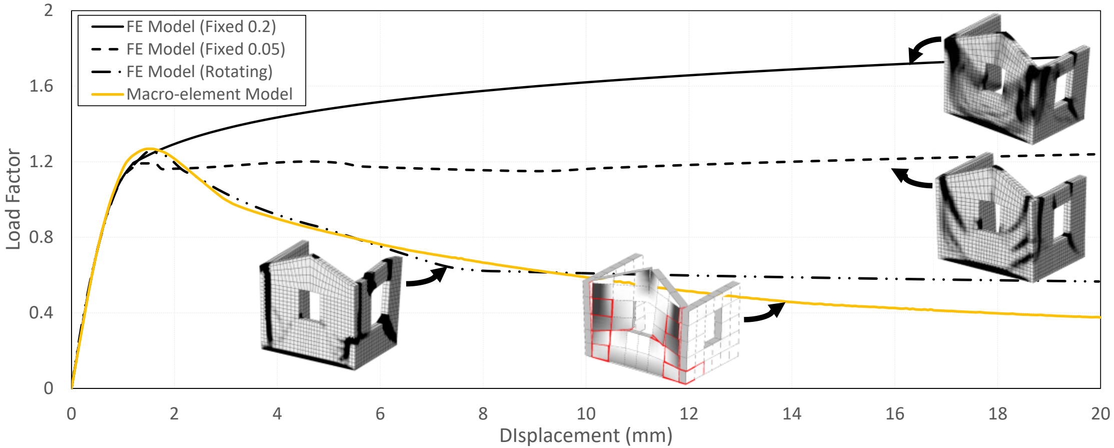

C. Chácara, N. Mendes, and P. B. Lourenço, "Simulation of Shake Table Tests on Out-of-Plane Masonry Buildings. Part (IV): Macro and Micro FEM Based Approaches," International Journal of Architectural Heritage, vol. 11, pp. 103-116, (2017).

C. Chácara, F. Cannizzaro, B. Pantò, I. Caliò, and P. B. Lourenço, "Assessment of the Dynamic Response of Unreinforced Masonry Structures using a Macro-Element Modelling Approach," Earthquake Engineering and Structural Dynamics, vol. 47, pp. 2426-46, (2018).

nonlinear dynamic time-history analyses

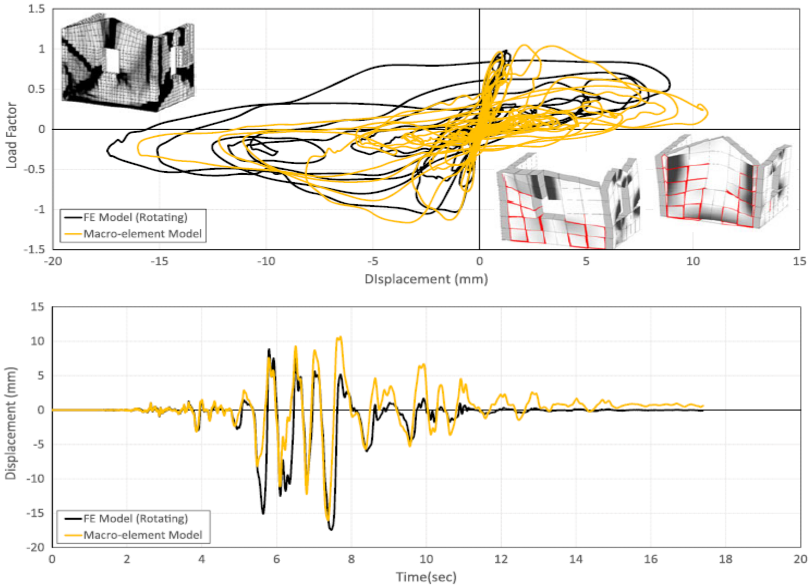

(A)

(B)

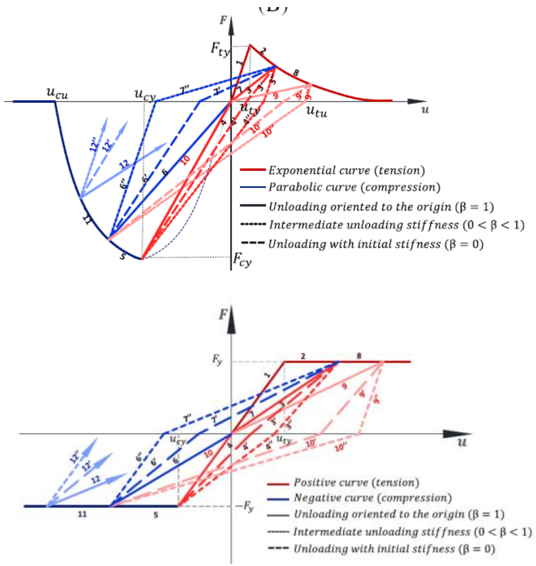

Chácara C, Cannizzaro F, Pantò B, Caliò I, Lourenço PB. Assessment of the dynamic response of unreinforced masonry structures using a macroelement modeling approach. Earthquake Engng Struct Dyn. 2018;1–21.

The application of the DMEM to a masonry arch bridge

INFRASTRUTTURA

PONTI FERROVIARI AD ARCO

Metodologia per l'analisi tridimensionale non lineare

di **Ivo CALIÒ**, **Francesco CANNIZZARO**, **Giuseppe OCCHIPINTI**,
Bartolomeo PANTÒ, **Davide RAPICAVOLI**, **Domenico D'URSO**
Università degli Studi di Catania, Dipartimento di Ingegneria Civile e Architettura (DICAR)

e **Gabriele PISANELLI**, **Gabriele SPIROLAZZI**, **Rocco ZURLO**
RFI - Direzione Territoriale Produzione Milano - Struttura Organizzativa Ingegneria

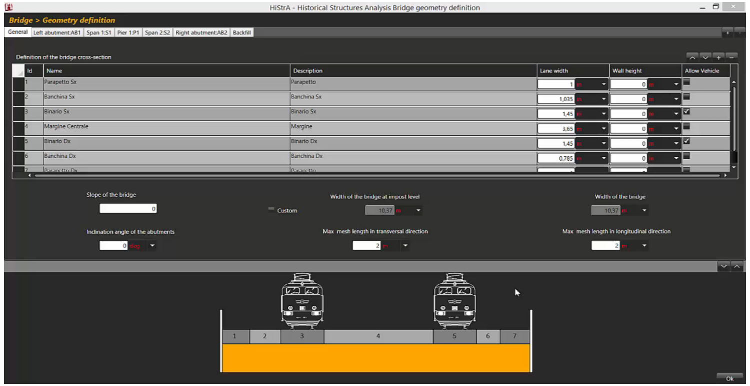

HiStrA - Historical Structures Analysis Bridge geometry definition

Bridge > Geometry definition

Definition of the bridge cross-section

Id	Name	Description	Lane width	Wall height	Allow Vehicle
1	Parapetto Sx	Parapetto	1 m	0 m	☐
2	Banchina Sx	Banchina Sx	1,035 m	0 m	☐
3	Binario Sx	Binario Sx	1,45 m	0 m	☑
4	Margine Centrale	Margine	3,65 m	0 m	☐
5	Binario Dx	Binario Dx	1,45 m	0 m	☑
6	Banchina Dx	Banchina Dx	0,785 m	0 m	☐
7	Parapetto Dx	Parapetto			☐

Slope of the bridge: 0

☐ Custom

Width of the bridge at impost level: 10,37 m

Width of the bridge: 10,37 m

Inclination angle of the abutments: 0 deg

Max mesh length in transversal direction: 2 m

Max mesh length in longitudinal direction: 2 m

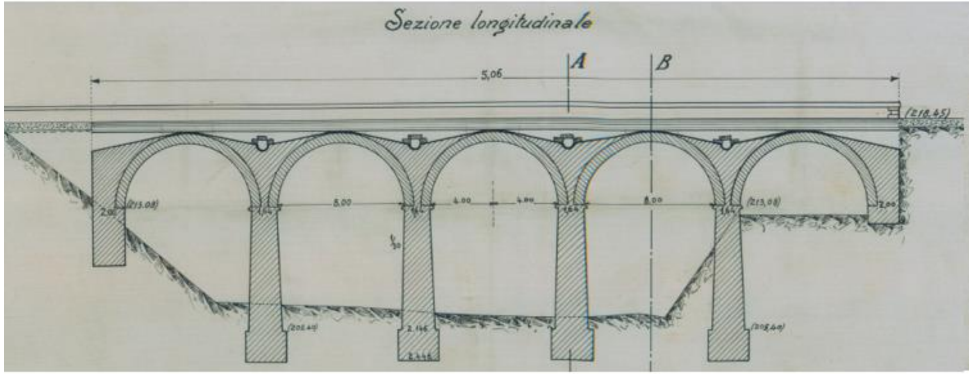

The application of the DMEM to a masonry arch bridge

An simple and innovative parametric input allows an easy and fast implementation of the entire model including the load distributions

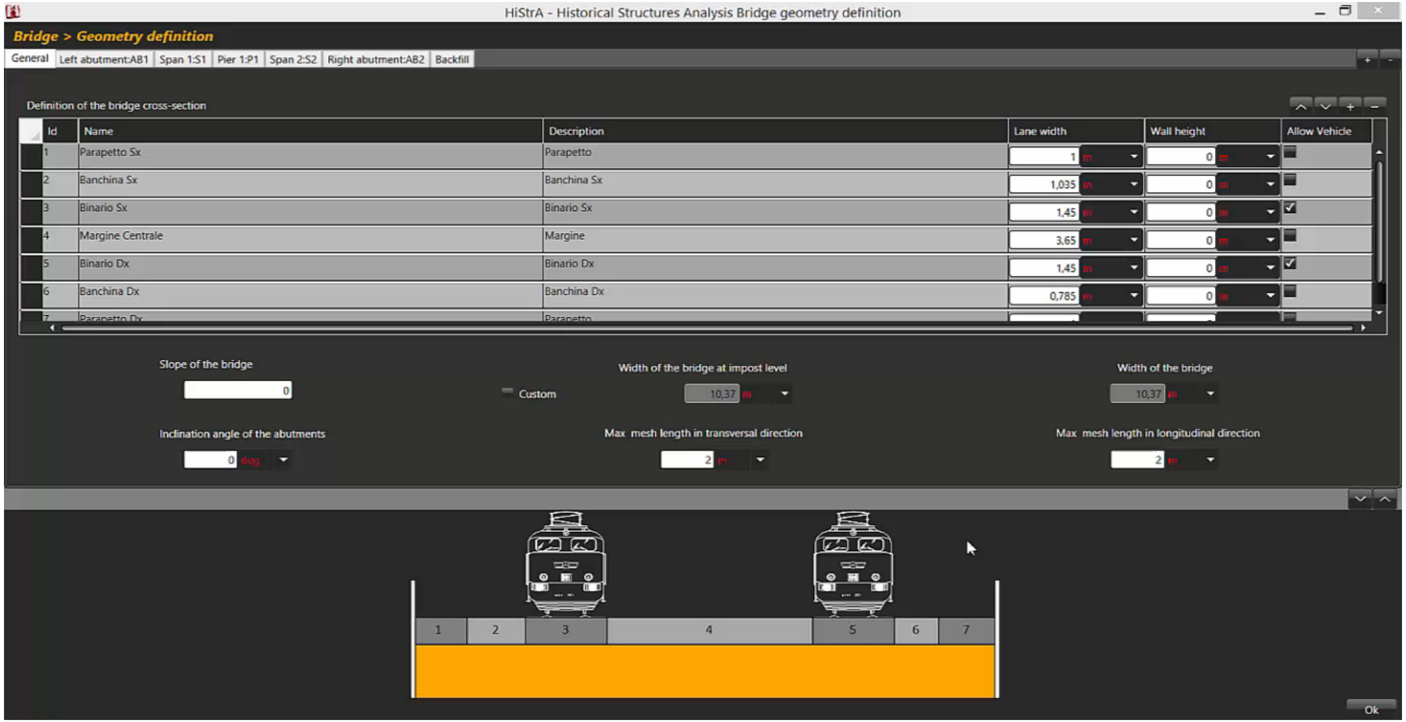

Definition of the bridge cross-section

Id	Name	Description	Lane width	Wall height	Allow Vehicle
1	Parapetto Sx	Parapetto	1 m	0 m	☐
2	Banchina Sx	Banchina Sx	1,035 m	0 m	☐
3	Binario Sx	Binario Sx	1,45 m	0 m	☑
4	Margine Centrale	Margine	3,65 m	0 m	☐
5	Binario Dx	Binario Dx	1,45 m	0 m	☑
6	Banchina Dx	Banchina Dx	0,785 m	0 m	☐
7	Parapetto Dx	Parapetto			☐

Slope of the bridge: 0

☐ Custom

Width of the bridge at impost level: 10,37 m

Width of the bridge: 10,37 m

Inclination angle of the abutments: 0 deg

Max mesh length in transversal direction: 2 m

Max mesh length in longitudinal direction: 2 m

numerical validation: DMEM versus FEM

Elements	f_m [MPa]	τ_0 [MPa]	E [MPa]	G [MPa]	w [kN/m^3]	f_t [MPa]	G_{ft} [N/mm]	G_{fc} [N/mm]
Abutment, pier, spandrel wall	5.8	0.4	2060	860	22	0.12	0.02	100
Masonry arches	2.6	0.3	1200	500	18	0.12	0.02	100
Backing, fill material, ballast	1.1	0.05	700	290	19	0.05	∞	100

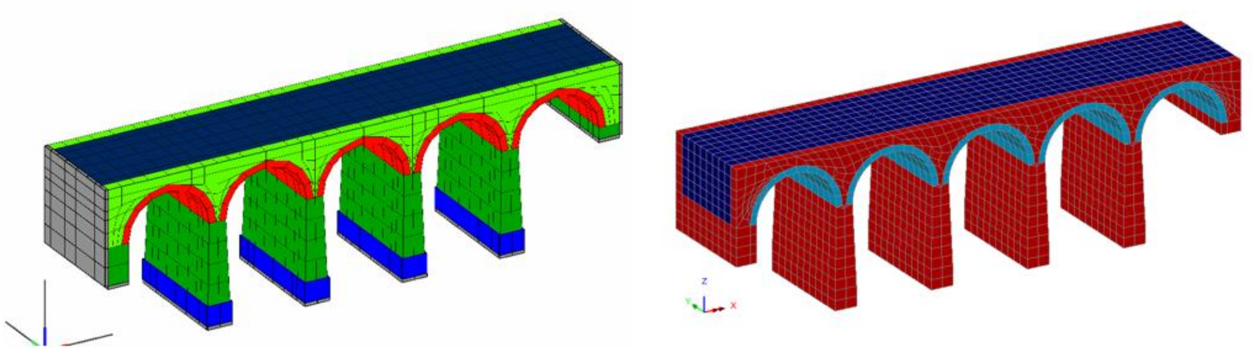

(a)

(b)

3D general views of (a) HISTRA and (b) LUSAS models.

Linear elastic numerical validation DMEM versus FEM

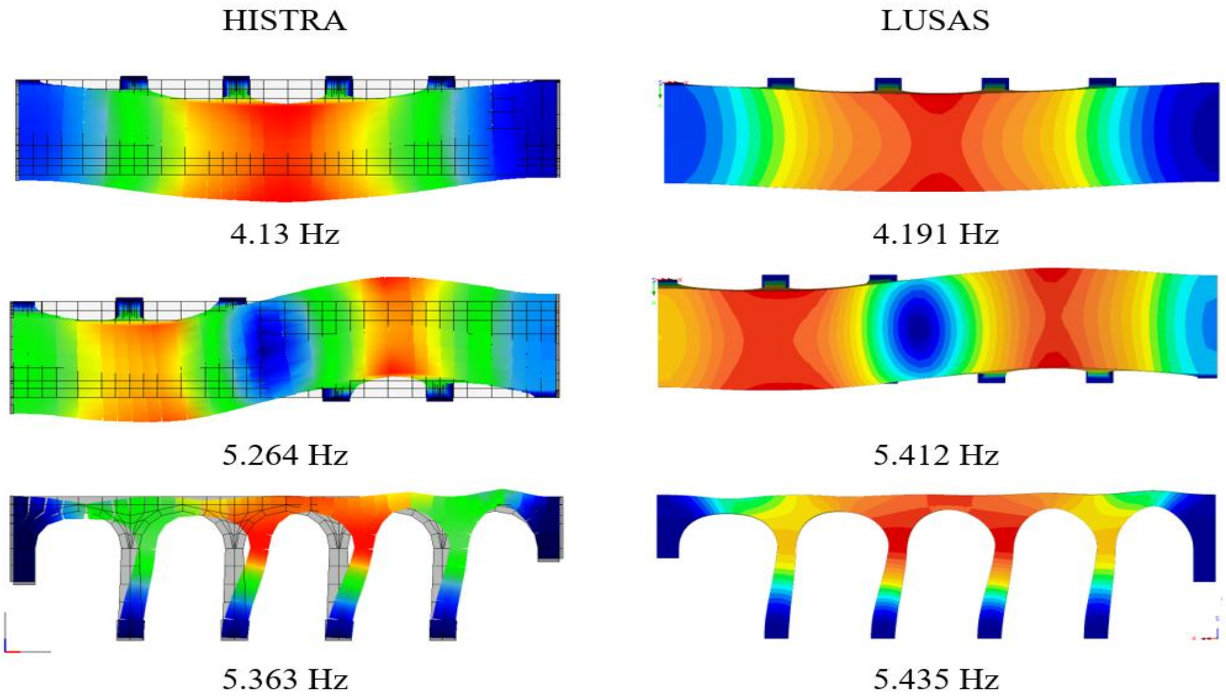

HiStrA-Bridge versus LUSAS. Comparison between the first three vibration frequencies and the corresponding vibration modes.

Nonlinear Static push-over analyses for vertical loads HiStrA / LUSAs

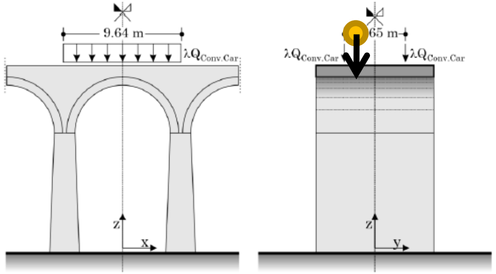

Figure 7: Scheme of the line loads distribution

Figure 9. Push-down comparison. DMEM (a) versus FEM (b), damage scenario, frontal and 3D-view.

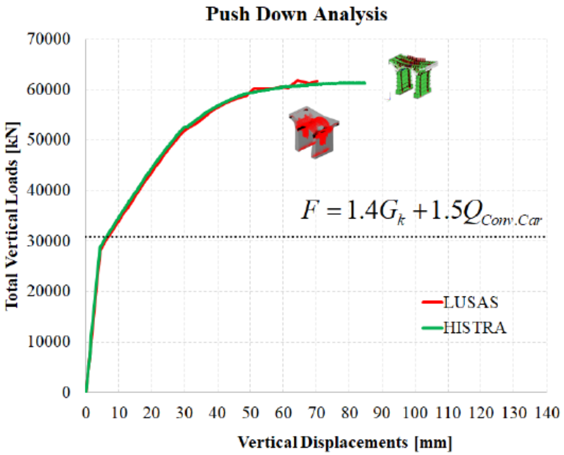

FEM
Shear damage is related to tensile strength

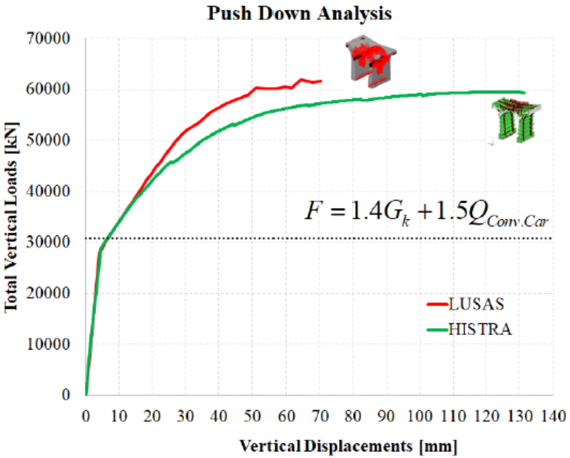

DMEM
Shear damage is related to the shear constitutive law

Nonlinear Static push-over analyses for vertical loads for the whole bridge DMEM versus FEM

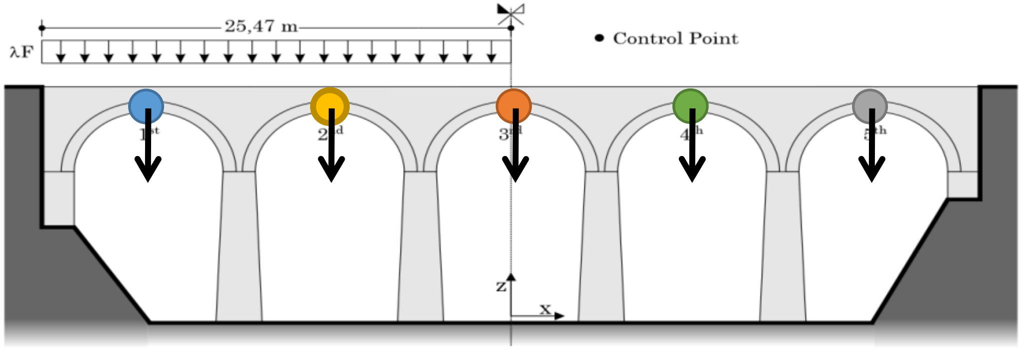

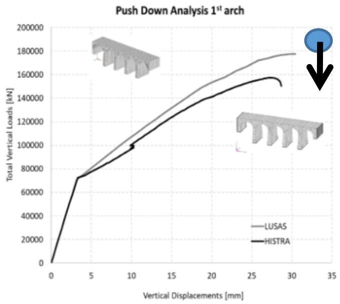
Push Down Analysis 1st arch

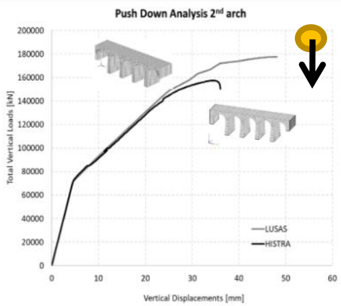
Push Down Analysis 2nd arch

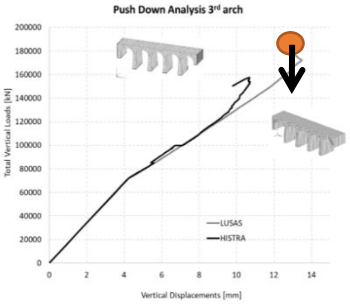
Push Down Analysis 3rd arch

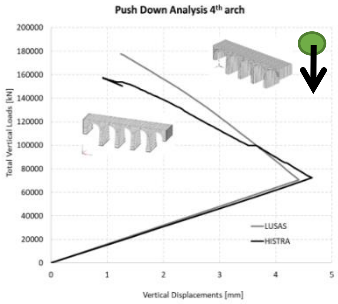
Push Down Analysis 4th arch

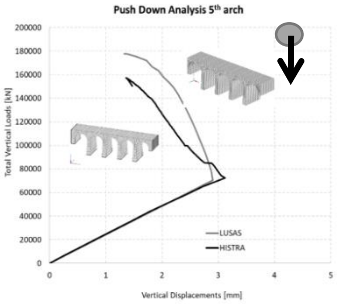
Push Down Analysis 5th arch

Nonlinear Static push-over analyses for vertical loads for the whole bridge DMEM versus FEM

Ultimate Compressive Stress Scenario [MPa]

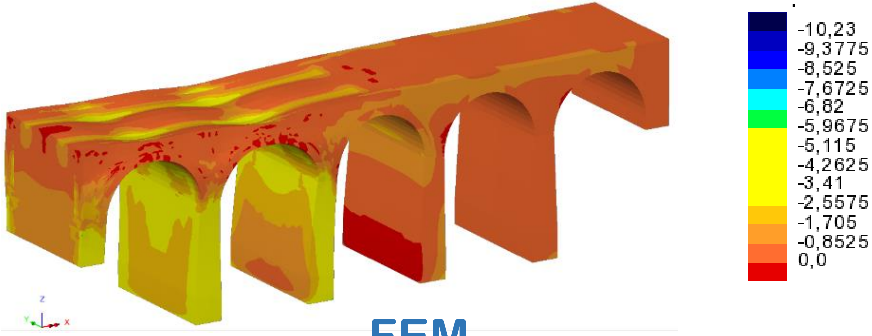

DMEM

FEM

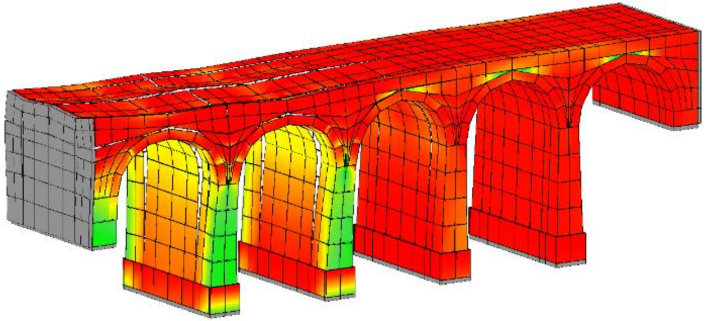

Nonlinear analyses for different load positions

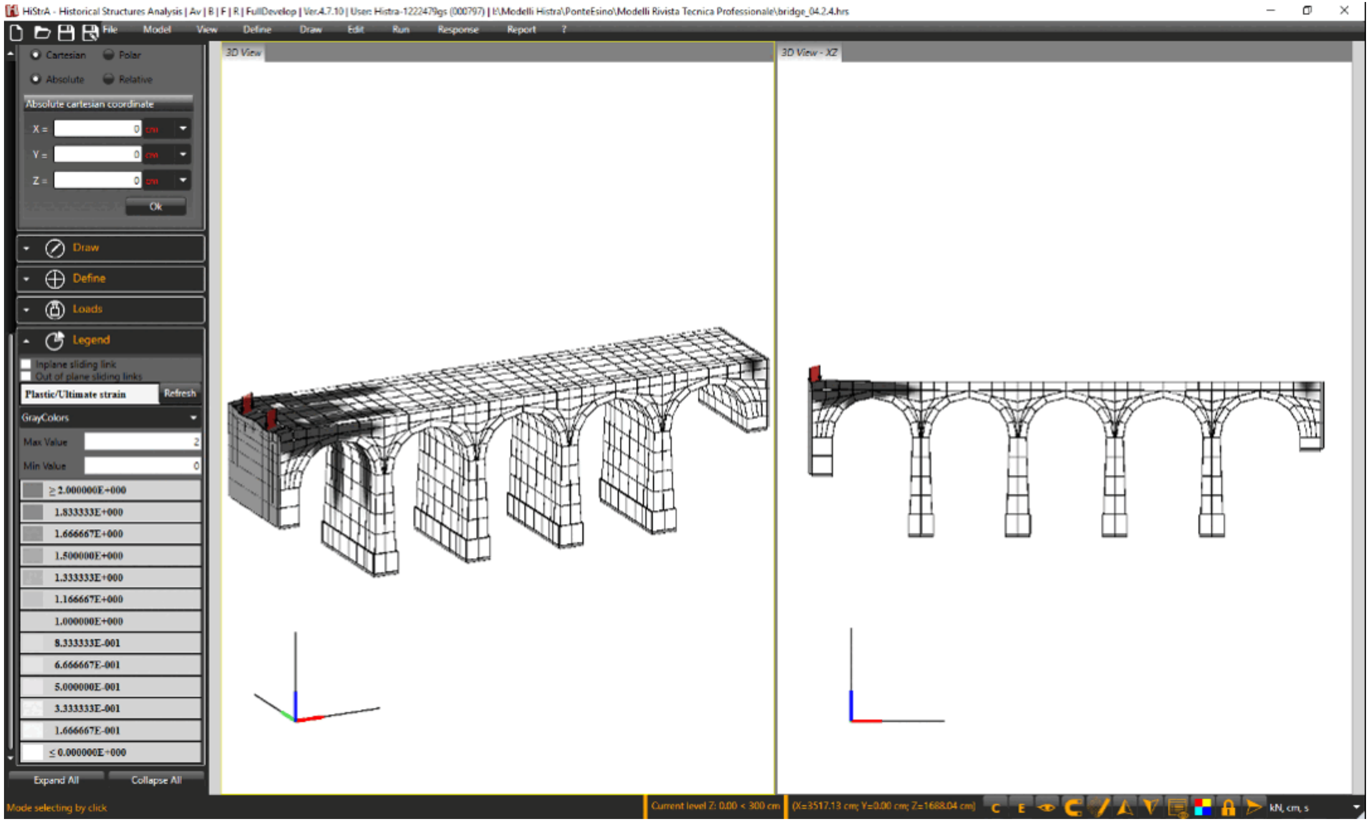

HiStrA - Historical Structures Analysis | Av | B | F | R | FullDevelop | Ver.4.7.10 | User: Histra-1222479gs (000797) | I:\Modelli Histra\PonteEsino\Modelli Rivista Tecnica Professionale\bridge_04.2.4.hrs

● Cartesian ○ Polar

● Absolute ○ Relative

Absolute cartesian coordinate

X = 0 cm

Y = 0 cm

Z = 0 cm

☐ Inplane sliding link

☐ Out of plane sliding links

Plastic/Ultimate strain

GrayColors

Max Value 2

Min Value 0

▨	≥ 2.000000E+000
▨	1.833333E+000
▨	1.666667E+000
▨	1.500000E+000
▨	1.333333E+000
▨	1.166667E+000
▨	1.000000E+000
▨	8.333333E-001
▨	6.666667E-001
▨	5.000000E-001
▨	3.333333E-001
▨	1.666667E-001
☐	≤ 0.000000E+000

Mode selecting by click

Current level Z: 0.00 < 300 cm

(X=3517.13 cm; Y=0.00 cm; Z=1688.04 cm)

kN, cm, s

Example of application of macro-element modelling strategy to a curved masonry arch Bridge

Materials
🟦 Foundations
🟩 Piers
🟥 Arches
🟫 Backfill
🟦 Fill

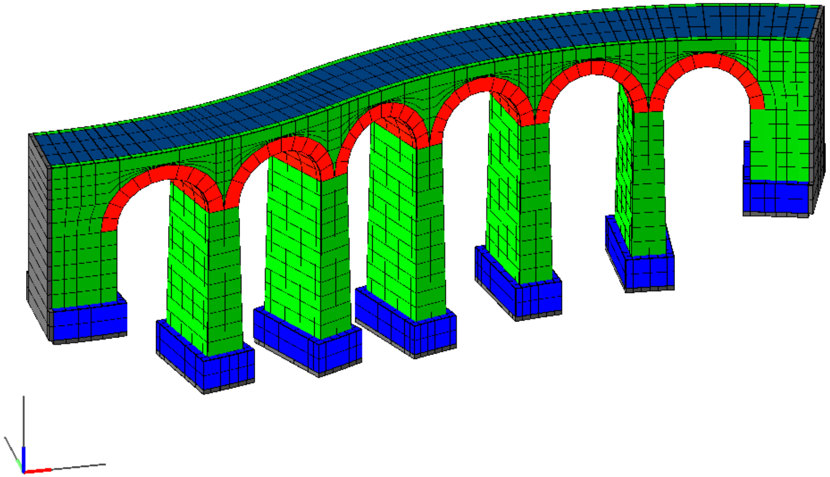

This is a numerical simulation of a masonry arch bridge. The total Length is 68.5 m, the cross-section width is 5.3m.

The bridge has 6 circular arches.
Span length L= 6.0 m and rise f=3.0 m,
Piers heigth = 10.0 – 11.0 – 12.0 – 11.0 – 10.0 m,
Abutment height = 5.0 m.

The bridge has two curvatures of R=40.0m

Material	E [MPa]	G [MPa]	f_t [MPa]	f_c [MPa]	G_t [N/mm]	G_c [N/mm]	τ_0 [MPa]	c [MPa]	μ	W $[kN/m^3]$	Constitutive Laws
Foundations, Piers, Arches	1800	600	0.1	4.6	0.01	3.0	0.13	0.13	0.6	18	Flexional: Elastic with Linear Softening Diagonal Shear: Turnsek-Cacovic Sliding Shear: Mohr-Coulomb
Backfill, Fill	300	115	0.025	0.5	-	-	-	-	-	18	Flexional: Elastic Perfectly Plastic Diagonal Shear: Elastic Sliding Shear: Elastic
Friction Interfaces	300	115	0.01	1	-	-	-	0.0	0.6	-	Flexional: Elastic Perfectly Plastic Sliding Mohr Coulomb

Application of Macro-element modelling strategy to a curved masonry arch Bridge

Materials	
🟦	Foundations
🟩	Piers
🟥	Arches
🟫	Backfill
🟪	Fill
🟦	Fill

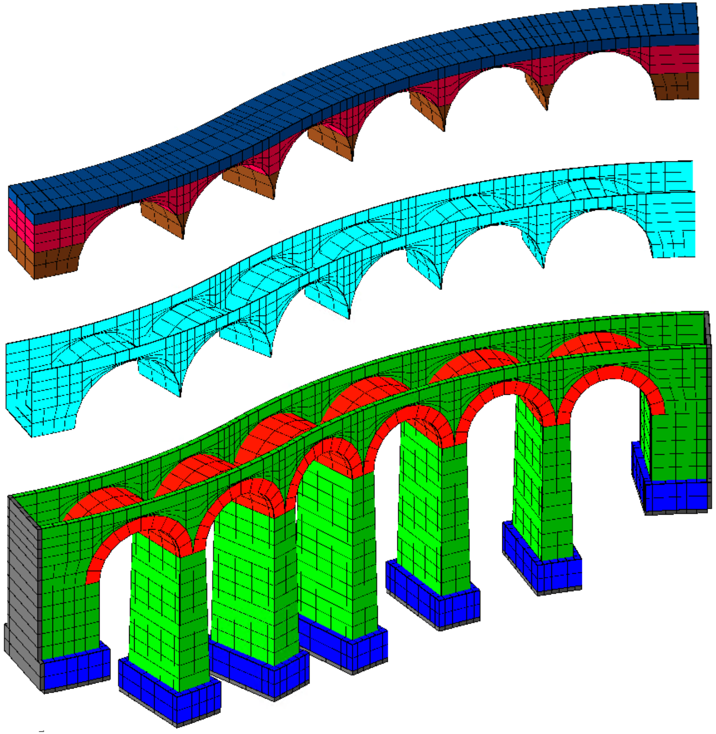

Fill & Backfill

Friction interfaces

Foundations, Piers, Arches

Application of Macro-element modelling strategy to a curved masonry arch Bridge

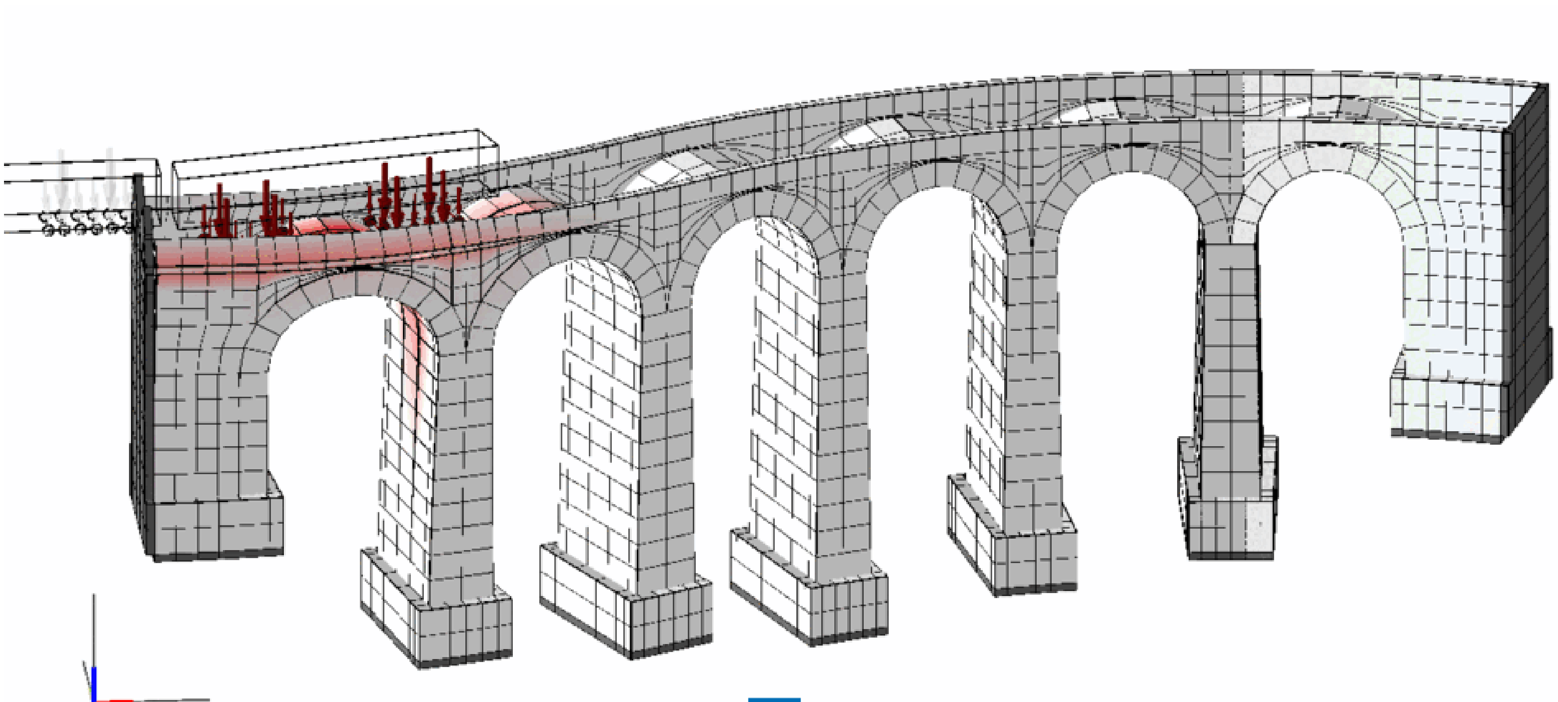

HISTRA FOR BRIDGES

Application of Macro-element modelling strategy to Masonry Arch Curved Bridge

the collapse load multiplier λ as a function of the load position

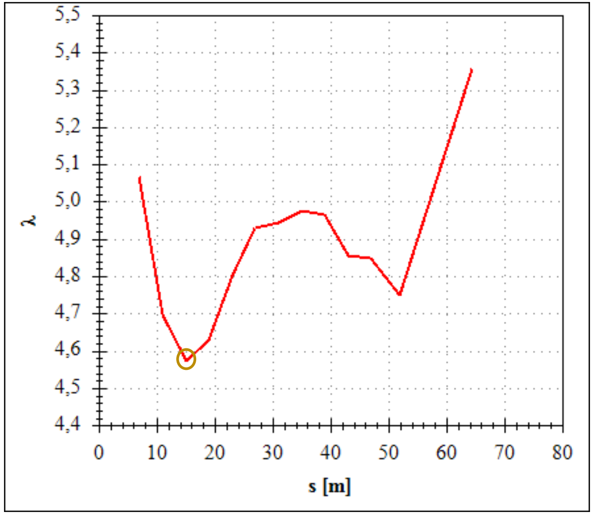

○ x=15.0 m
λ=4.57

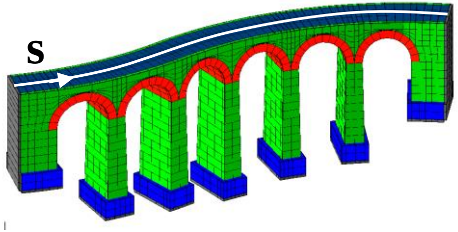

Pushdown curve at position x= 15.0m

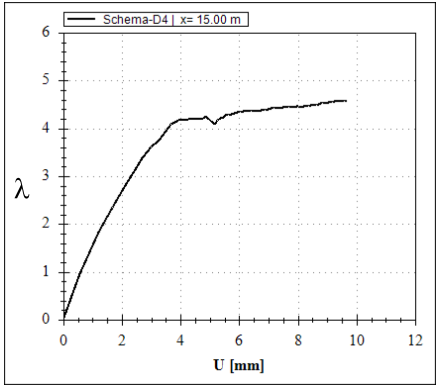

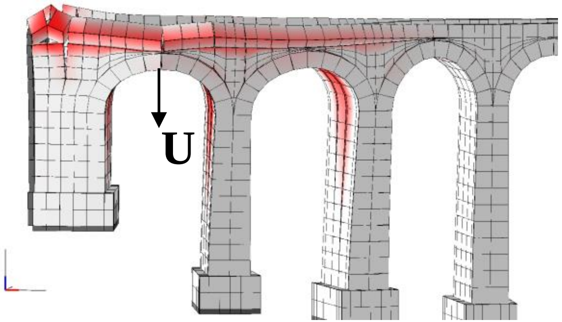

The modelling of a steel ring reinforcement of the arches

The bridge has been retrofitted in 1980 with the introduction of a concrete layer at the intrados of the vaults confined by an external steel corrugated thick plate used as formworks. The new structure was founded on a new reinforced concrete enlargement of the existing masonry foundation.

The modelling of a steel ring reinforcement of the arches

Unstrengthened configuration

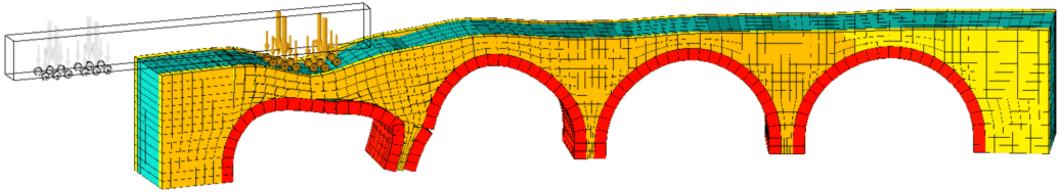

Strengthened configuration

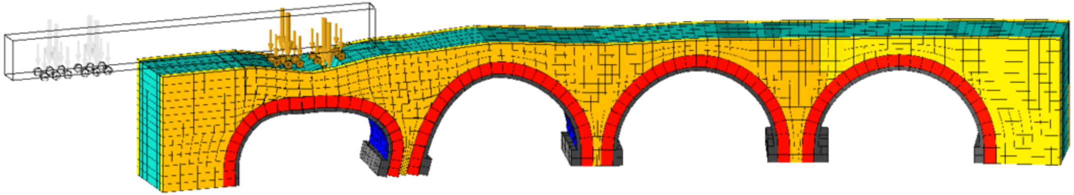

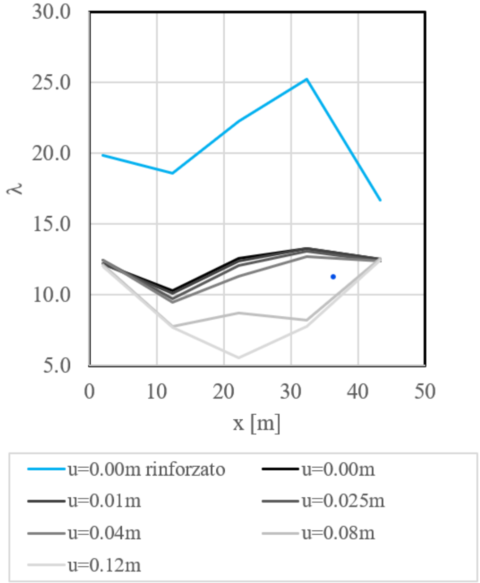

The modelling of a steel ring reinforcement of the arches

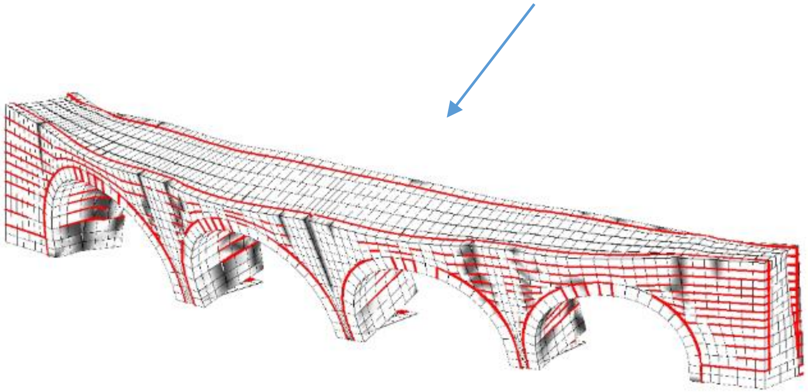

Unstrengthened configuration

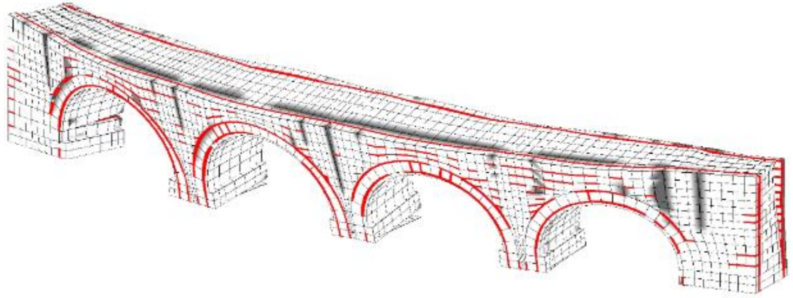

Strengthened configuration

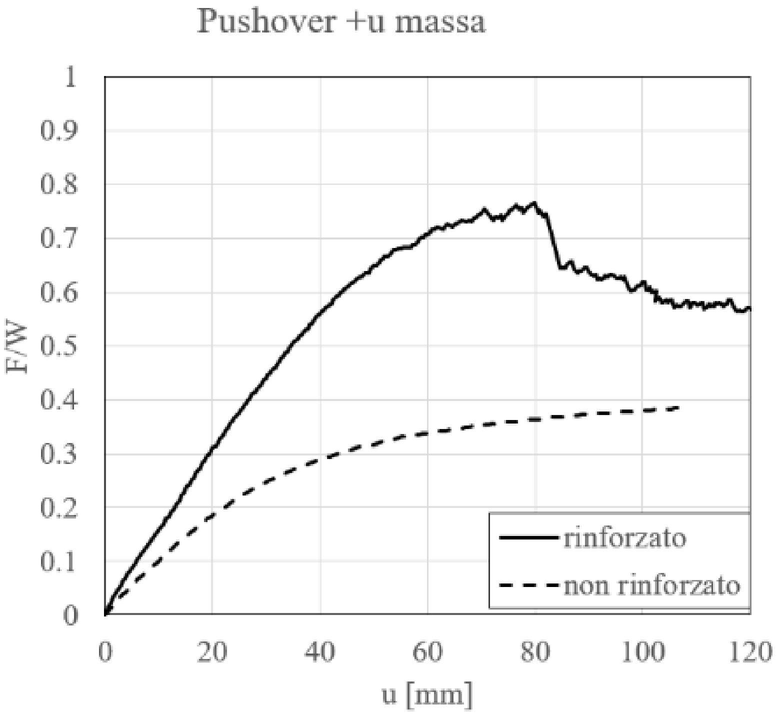

The modelling of a steel ring reinforcement of the arches

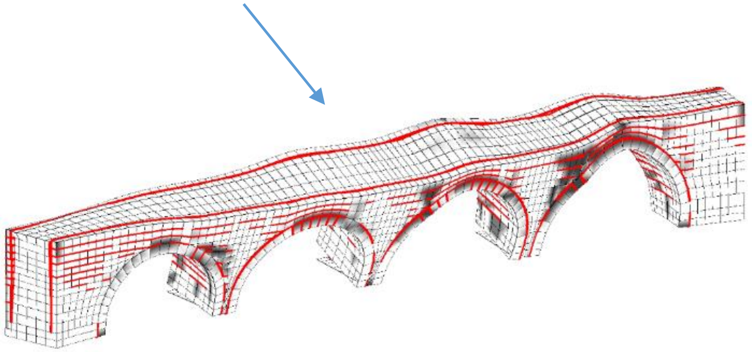

Unstrengthened configuration

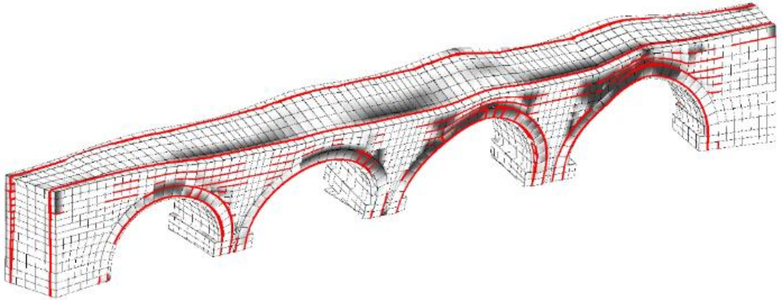

Strengthened configuration

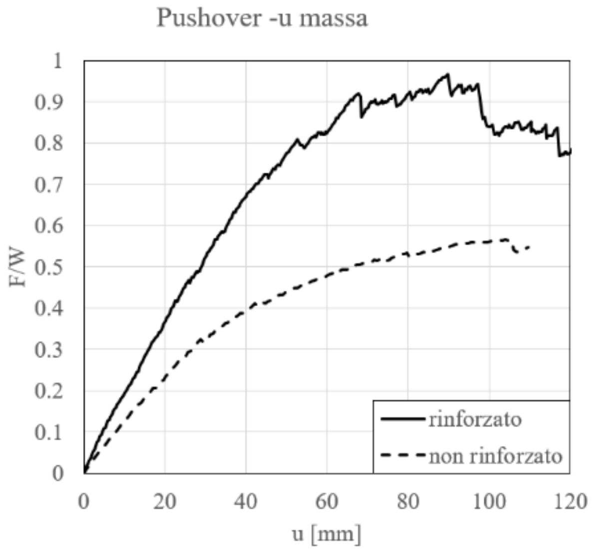

Formulation of a new the 3D Solid Macro-Element: Kinematics

A solid discrete macro-element

Work in progress …

Marcello Falco, Davide Rapicavoli, Ivo Caliò et al …

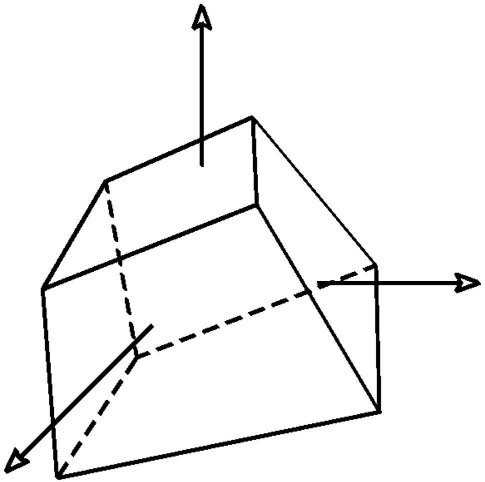

the new discrete element has the shape of an irregular hexahedron with continuous interfaces and a number of degrees of freedom varying from 6 to 18 according to the desired kinematics

The shear deformation: the kinematics

Virtual Macro-Element in the Intrinsic Coordinates Space

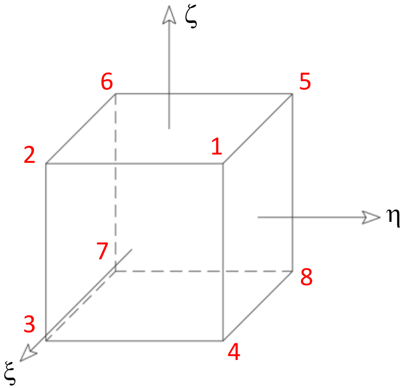

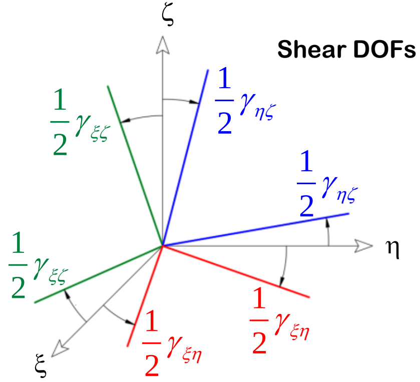

Shape Functions

$$M_i(\xi,\eta,\zeta)=\frac{(1+\xi_i\xi)(1+\eta_i\eta)(1+\zeta_i\zeta)}{8}$$

$$\frac{\partial M_i}{\partial \xi}=\xi_i\frac{(1+\eta_i\eta)(1+\zeta_i\zeta)}{8}$$

$$\frac{\partial M_i}{\partial \eta}=\eta_i\frac{(1+\xi_i\xi)(1+\zeta_i\zeta)}{8}$$

$$\frac{\partial M_i}{\partial \zeta}=\zeta_i\frac{(1+\xi_i\xi)(1+\eta_i\eta)}{8}$$

i	ξ_i	η_i	ζ_i
1	1	1	1
2	1	-1	1
3	1	-1	-1
4	1	1	-1
5	-1	1	1
6	-1	-1	1
7	-1	-1	-1
8	-1	1	-1

Real Macro-Element in the Cartesian Coordinates Space

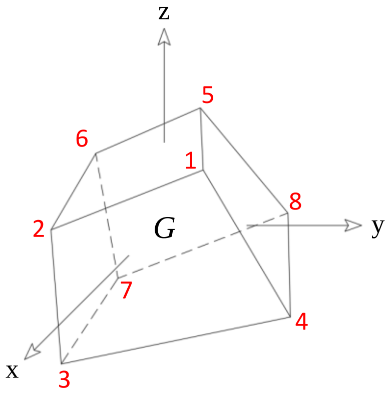

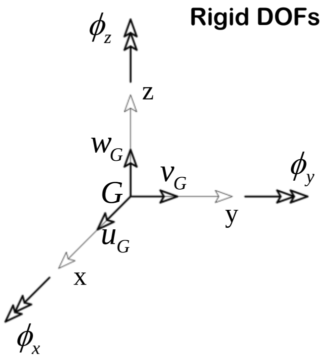

Complete Vector of DOFs

$$\Gamma^T=\Big[\underbrace{u_G \quad v_G \quad w_G \quad \phi_x \quad \phi_y \quad \phi_z}_{\textbf{Rigid DOFs}} \quad \underbrace{\gamma_{\xi\eta} \quad \gamma_{\xi\zeta} \quad \gamma_{\eta\zeta}}_{\textbf{Shear DOFs}}\Big]$$

The shear deformation: the kinematics

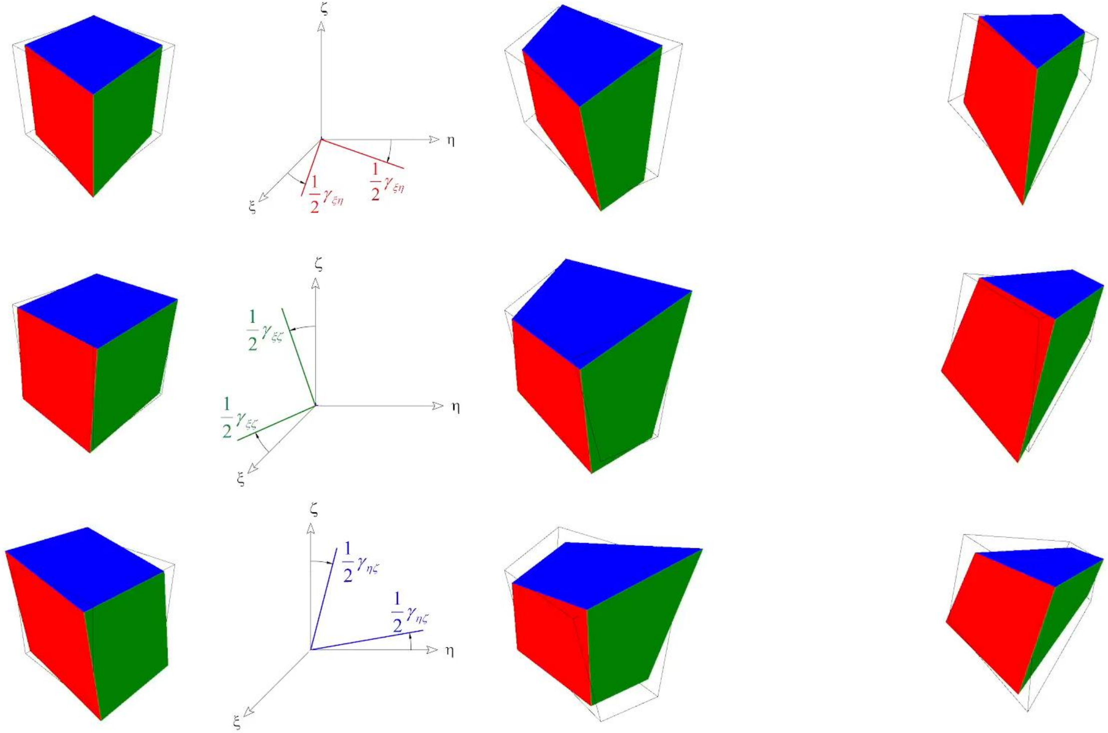

Regular **slightly irregular** **very irregular**

The shear deformation: the kinematics

Displacement $\Delta\vec{\xi}$ of the point $\vec{\xi}$ in the Intrinsic Coordinates Space

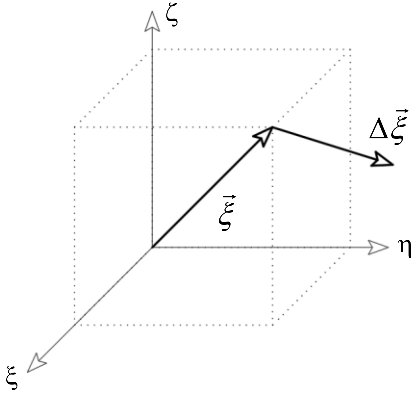

$$\vec{\xi} \equiv (\xi, \eta, \zeta)$$

$$\Delta\vec{\xi} \equiv \left(\frac{1}{2}\gamma_{\xi\eta}\eta + \frac{1}{2}\gamma_{\xi\zeta}\zeta,\ \frac{1}{2}\gamma_{\xi\eta}\xi + \frac{1}{2}\gamma_{\eta\zeta}\zeta,\ \frac{1}{2}\gamma_{\xi\zeta}\xi + \frac{1}{2}\gamma_{\eta\zeta}\eta \right)$$

Displacement $\vec{u}$ of the point $\vec{x}$ in the Cartesian Coordinates Space due to the Shear DOFs

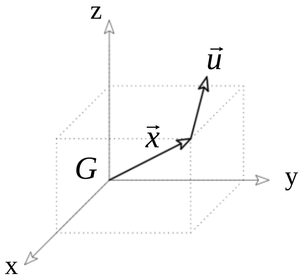

$$\vec{x}(\xi, \eta, \zeta) = \sum_{i=1}^{8} \vec{x}_i M_i (\xi, \eta, \zeta)$$

$$\vec{u}(\xi, \eta, \zeta) = \frac{1}{2}\gamma_{\xi\eta}\left(\xi \frac{\partial \vec{x}}{\partial \eta} + \eta \frac{\partial \vec{x}}{\partial \xi} \right) + \\ + \frac{1}{2}\gamma_{\xi\zeta}\left(\xi \frac{\partial \vec{x}}{\partial \zeta} + \zeta \frac{\partial \vec{x}}{\partial \xi} \right) + \\ + \frac{1}{2}\gamma_{\eta\zeta}\left(\eta \frac{\partial \vec{x}}{\partial \zeta} + \zeta \frac{\partial \vec{x}}{\partial \eta} \right)$$

Further degrees of freedom accounting for Poisson effect

Displacement $\Delta\vec{\xi}$ of the point $\vec{\xi}$ in the Intrinsic Coordinates Space

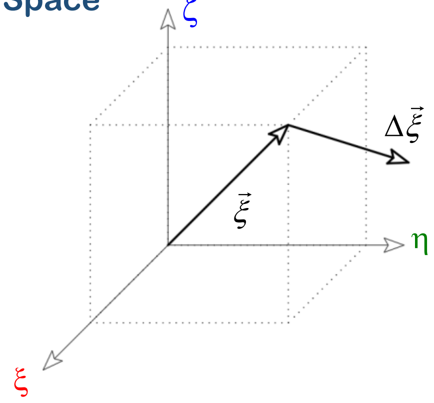

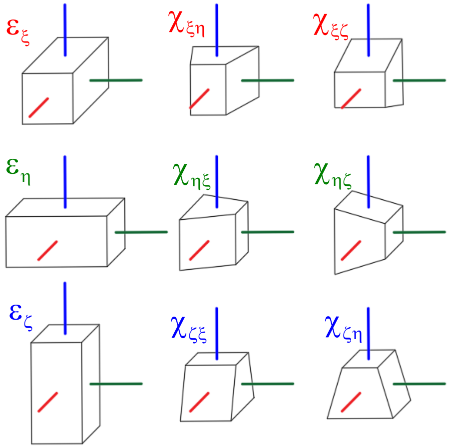

$$\vec{\xi} \equiv (\xi, \eta, \zeta)$$

$$\Delta\vec{\xi} = \Delta\vec{\xi}_{shear} + \Delta\vec{\xi}_{dilatation} + \Delta\vec{\xi}_{curvature}$$

$$\Delta\vec{\xi}_{dilatation} \equiv \left(\varepsilon_{\xi}\xi,\ \varepsilon_{\eta}\eta,\ \varepsilon_{\zeta}\zeta\right)$$

$$\Delta\vec{\xi}_{curvature} \equiv \left(-\frac{1}{2}\xi\left(\chi_{\eta\xi}\eta + \chi_{\zeta\xi}\zeta\right), -\frac{1}{2}\eta\left(\chi_{\xi\eta}\xi + \chi_{\zeta\eta}\zeta\right), -\frac{1}{2}\zeta\left(\chi_{\xi\zeta}\xi + \chi_{\eta\zeta}\eta\right)\right)$$

Displacement $\vec{u}$ of the point $\vec{x}$ in the Cartesian Coordinates Space due to the dilatation and curvature DOFs

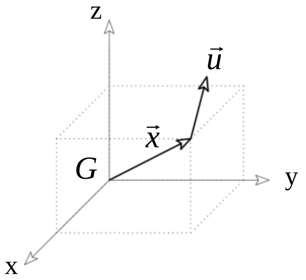

$$\vec{x}(\xi,\eta,\zeta) = \sum_{i=1}^{8} \vec{x}_i M_i(\xi,\eta,\zeta)$$

$$\vec{u}(\xi,\eta,\zeta) = \vec{u}_{shear}(\xi,\eta,\zeta) + \vec{u}_{dilatation}(\xi,\eta,\zeta) + \vec{u}_{curvature}(\xi,\eta,\zeta)$$

$$\vec{u}_{dilatation}(\xi,\eta,\zeta) = \varepsilon_{\xi}\xi\frac{\partial\vec{x}}{\partial\xi} + \varepsilon_{\eta}\eta\frac{\partial\vec{x}}{\partial\eta} + \varepsilon_{\zeta}\zeta\frac{\partial\vec{x}}{\partial\zeta}$$

$$\vec{u}_{curvature}(\xi,\eta,\zeta) = -\frac{1}{2}\xi\left(\chi_{\xi\eta}\eta\frac{\partial\vec{x}}{\partial\eta} + \chi_{\xi\zeta}\zeta\frac{\partial\vec{x}}{\partial\zeta}\right)$$

$$-\frac{1}{2}\eta\left(\chi_{\eta\xi}\xi\frac{\partial\vec{x}}{\partial\xi} + \chi_{\eta\zeta}\zeta\frac{\partial\vec{x}}{\partial\zeta}\right)$$

$$-\frac{1}{2}\zeta\left(\chi_{\zeta\xi}\xi\frac{\partial\vec{x}}{\partial\xi} + \chi_{\zeta\eta}\eta\frac{\partial\vec{x}}{\partial\eta}\right)$$

Further degrees of freedom accounting for Poisson effect: representation on the regular element

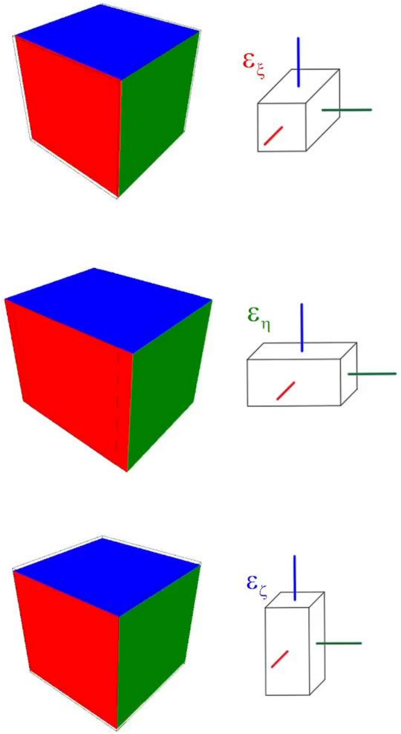

Dilatation

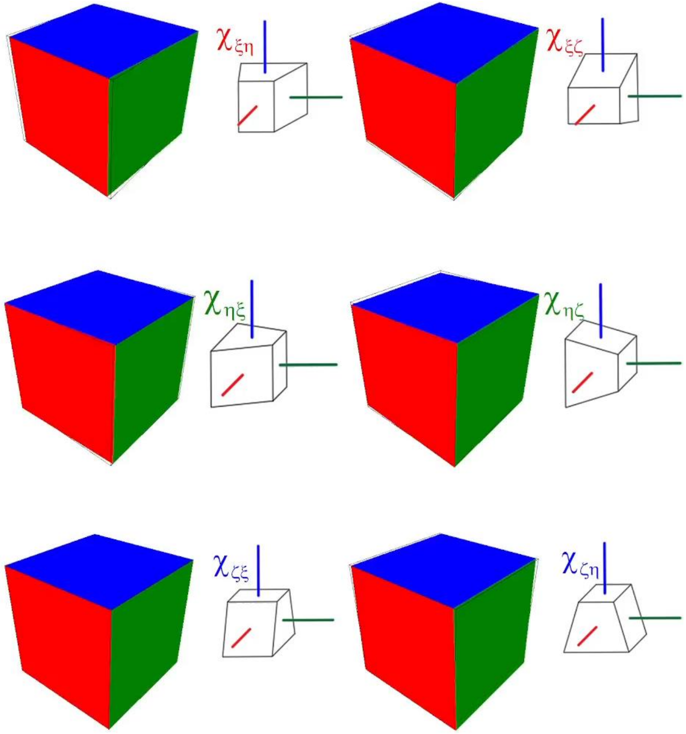

curvatures

Application of the solid macro-element to curved structures a first validation

Validation in dynamic elastic field: FEM vs DMEM models

LUSAS

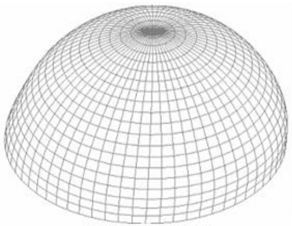
First modal shape
(T1 = T2 = 0,0217 sec)

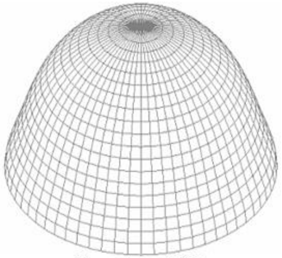
Second modal shape
(T3 = 0,0164 sec)

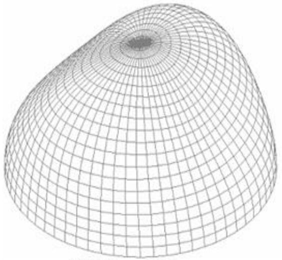
Third modal shape
(T4 = T5 = 0,0142 sec)

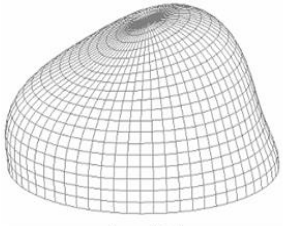
Fourth modal shape
(T6 = T7 = 0,0141 sec)

HISTRA
FOR BRIDGES

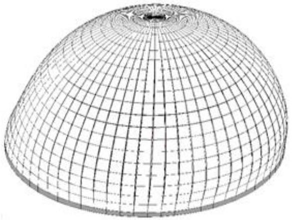
First modal shape
(T1 = T2 = 0,0212 sec)

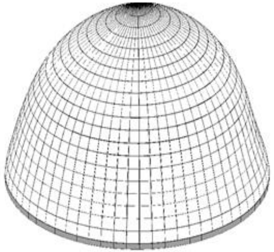
Second modal shape
(T3 = 0,0158 sec)

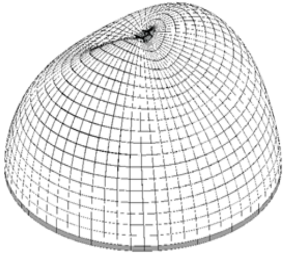
Third modal shape
(T4 = T5 = 0,0148 sec)

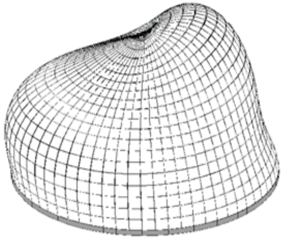
Fourth modal shape
(T6 = T7 = 0,0143 sec)

Application of the solid macro-element to curved structures a first validation

The third application is a validation in the non linear field based on experimental test performed by Foraboschi (2006) of a masonry hemispherical dome [*]

The dome has a circular opening of
0.20 m, the inner radius is 2.2 m,
with a thickness of 12 cm.
The vertical load is applied to a ring
around the hole.

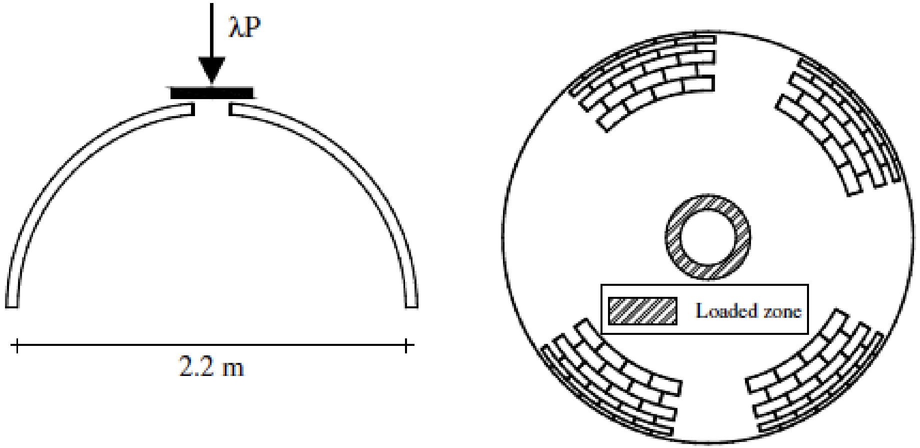

E [MPa]	ν	γ[kN/m^3]	σ_t [MPa]	σ_c [MPa]	c [MPa]	μ
850	0.25	20	0.07	1.9	0.12	0.37

[*] P., Foraboschi, Masonry structures externally reinforced with FRP strips: tests at the collapse [in Italian], 2006. In: Proceedings of I Convegno Nazionale "Sperimentazioni su Materiali e Strutture", Venice.

Application of the solid macro-element to curved structures a first validation

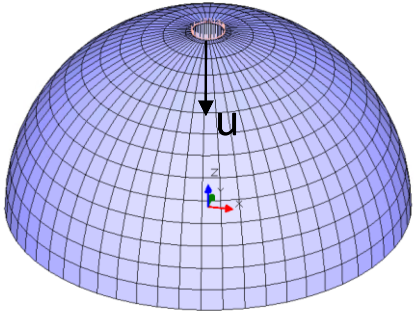

DMEM Solid model

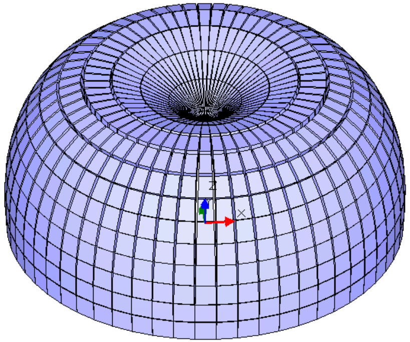

Displacements at 5 mm

Validation in non linear field:
FEM vs Limit Analysis vs DMEM models

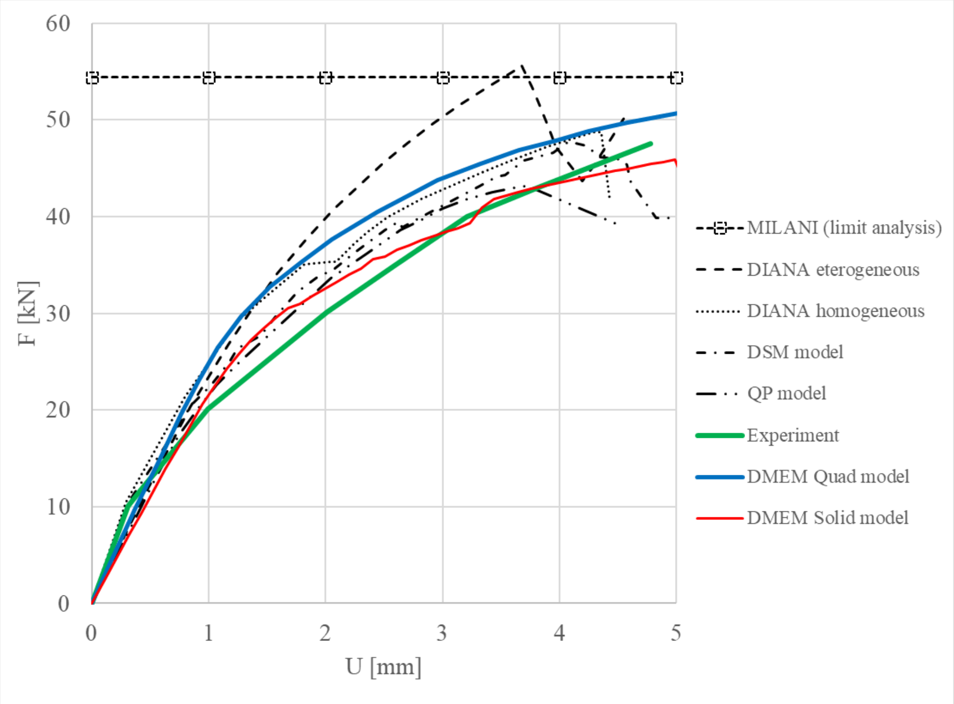

Conclusions

- A three-dimensional macro-element method (DMEM) has been presented and applied to a multi-span masonry railway arch bridges
- The DMEM allows a reliable simulation of the linear and nonlinear response of masonry bridges with a lower computational cost compared to classical nonlinear FEM analyses.
- The kinematics is related to the relative displacements between macro-elements measured at the interfaces and a strain deformation field associated to the element volume.
- A current development of a new discrete solid macro-element that overcomes some limitation of the previously introduced discrete macro-element has been introduced

Thanks